April 2013

Anti-Inflammatory System for Subcutaneous Biosensors

Catherine Anne Bannish
Worcester Polytechnic Institute

Keila M. Vazquez
Worcester Polytechnic Institute

Macauley Reardon Kenney
Worcester Polytechnic Institute

Follow this and additional works at: https://digitalcommons.wpi.edu/mqp-all

WORCESTER POLYTECHNIC INSTITUTE BIOMEDICAL ENGINEERING DEPARTMENT

Anti-Inflammatory System for Subcutaneous Biosensors

A Biomedical Engineering Major Qualifying Project

Catherine Bannish

Macauley Kenney

Keila Vazquez

4/25/2013

An anti-inflammatory system was created to reduce the inflammation and fibrotic scarring caused by a subcutaneous biosensor. This system was comprised of Titania nanotubes, chitosan hydrogel, and drug-releasing nanoparticles, and was aimed at reducing the adhesion and activation of macrophages. Testing suggests that the system reduces macrophage activity, and therefore the subsequent fibrotic encapsulation, in comparison to Ti foil, TiO2 nanotubes, and chitosan hydrogel acting in isolation.

Table of Contents

Table of Figures

Authorship

Abstract

Abstract—**An anti-inflammatory system was created to reduce the inflammation and fibrotic scarring caused by a subcutaneous biosensor. This system was comprised of Titania nanotubes, chitosan hydrogel, and drug-releasing nanoparticles, and was aimed at reducing the adhesion and activation of macrophages. Testing suggests that the system reduces macrophage activity, and therefore the subsequent fibrotic encapsulation, in comparison to Ti foil, TiO_2 nanotubes, and chitosan hydrogel acting in isolation.**

INTRODUCTION

The inflammatory response of the human body to the internal presence of foreign materials promotes the continued health and well-being of an individual. Unfortunately, in regards to subcutaneously implanted biosensors, this immune response disrupts the performance of the device's sensing capabilities by generating fibrotic tissue between the sensor and the body, as seen below in Fig. 1 [1][2]. The formation of this tissue matrix prevents the diffusion of metabolites to and from the sensor, resulting in a loss of metabolite sensitivity and eventual device failure [3].

In order to extend sensor functionality, the generation of fibrotic scarring must be delayed. Macrophages have been identified as a potential target to accomplishing this aim; they are the primary phagocytotic cell of the acute inflammatory response, and release pro-inflammatory cytokines to attract additional macrophages to the site upon activation [4][5].

This macrophage activation has been demonstrated to be reduced when exposed to TiO_2 nanotubes with a diameter of 70 nm as opposed to other metals or untreated titanium [6]. As Ti is considered to have superior biocompatibility, the enhanced biocompatibility of TiO_2 nanotubes suggests potential as an anti-inflammatory material when used in conjunction with other approaches such as anti-inflammatory drugs and hydrogels.

Therefore, the primary objective of this project is to investigate the viability of a TiO_2 nanotube anti-inflammatory system for a subcutaneous biosensor to (1) reduce macrophage activation at the site of biosensor insertion, (2) delay the inflammation response and fibrotic scarring development, and (3) extend the functional lifetime of that biosensor. To that aim, TiO_2 nanotubes were combined with a 1% chitosan solution and PLGA nanoparticle drug-delivery system and assessed on their combined ability to reduce the inflammatory response.
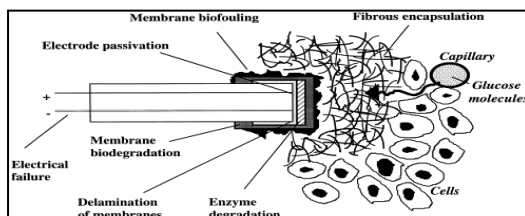
Fig. 1: Common inflammatory response impediments to biosensor functionality [1]

METHODS

Titania Nanotube Formation

Titanium foil (99% pure, 0.127mm thick) was obtained as a gift from Dr. Menon of Northeastern University. 3x5 cm pieces were ultrasonically cleaned in 100% isopropanol for 15mins. Samples were anodized at 15V in 0.25M hydrofluoric acid for 45mins and subsequently annealed in a tube furnace at 400°C for 4 hours. After annealing, Ti samples were rinsed with DI water, pure isopropanol, and ultrasonically cleaned in pure isopropanol for 15mins. Ti samples were cut into 0.5x0.5 cm squares and ultrasonically cleaned in pure ethanol before testing. Samples were characterized by SEM.

1% Chitosan Gel Production and Application

Chitosan was dissolved in 2% acetic acid solution with magnetic stirring for 2 hours. Chitosan coated samples were dipped in the solution prior to seeding and refrigerated at 4°C for 24 hours, and then placed in a 37°C oven until testing.

Macrophage Adhesion and Activation

Immortalized macrophages, harvested from C57bl/6 mice treated with J2 virus, and primary macrophages from C57 Black /6J (C57BL/6J) mice were a gift from UMASS Medical School. The macrophages were seeded onto a 48-well plate containing: 1% chitosan hydrogel, Ti foil, TiO_2 nanotubes, chitosan-coated Ti foil, chitosan-coated TiO_2 nanotubes, and a polystyrene control. Macrophages were tested for adherence, activation, and viability 1 and 7 days after seeding. 3 samples from each parameter were treated with 2.5% Phalloidin and 0.1% Hoechst stains to determine adhered population and viability. This analysis was conducted using an upright fluorescence microscope. The remaining samples were analyzed using SEM to observe adherence and activation.

Nanoparticle Release

Poly(lactic-co-glycolic acid) (PLGA) nanoparticles were created following a procedure by Chenna et al. and loaded with 12.5 μg/mL of Fluorescein isothiocyanate (FITC) [7]. 5 mg of the particles were mixed with 1.2% agarose and deposited into glass vials, three samples with 100 μL and three samples with 150μL, and left at 4°C for 1 hour. 10% PBS was added to the vials, 250μL and 300μL respectively, after gelation. PBS was collected after 1, 2, and 3 days, and then every alternate day until day 13. Equal amounts of PBS were collected and replaced. The collected PBS was analyzed using a Nanodrop 2000 Spectrophotometer to test the FITC absorbance.

RESULTS

Analysis of Nanotube Dimensions

Anodization produced TiO_2 nanotubes with an average outer diameter of 70 nm and an average inner diameter of 40 nm. The average length of the nanotubes was 200 nm measured

from the surface of the foil. The tubes covered the entirety of the foil surface.

Macrophage Viability

Chitosan-coated TiO_2 nanotubes seeded with primary macrophages noticeably demonstrated the lowest level of cells during fluorescence testing in comparison to all other samples at both time points, especially compared to the Ti foil and control. Wells seeded with immortalized macrophages were difficult to analyze due to cell proliferation.

Macrophage Adhesion and Activation

All samples demonstrated an amount of macrophage adhesion and activation, which was determined by cell morphology as shown in Fig. 2. Ti foil possessed the highest amount of adhesion and activation among the 1 day samples; chitosan-coated samples possessed the least with nearly all of the adhered macrophages remaining inactivated. After 7 days the chitosan-coated samples demonstrated minimal adhesion and activation in comparison to the non-chitosan coated samples and the control. Areas where the chitosan layer had torn were more attractive to macrophage adhesion; this was observed more often on Ti foil samples than TiO_2 nanotubes.
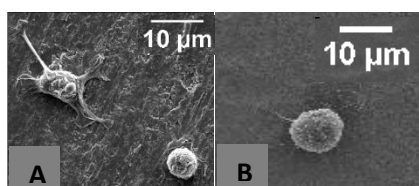
Fig. 2: (A) Day 1 Ti foil with activated (left) and inactivated (right) macrophages, (B) Day1 chitosan-coated TiO_2 nanotubes with an inactivated macrophage

Nanoparticle Release Study

The nanoparticle release study lasted 13 days. A plateau resulted in both well types at day 7 at a cumulative concentration of about 10μg/mL, as shown in Fig. 3.
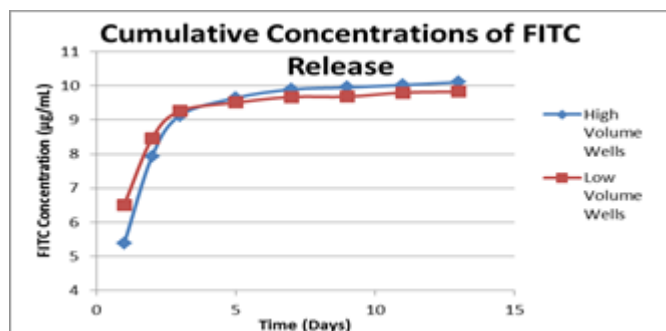
Fig. 3: The cumulative concentrations of FITC released over 13 days from PLGA nanoparticles in agarose

DISCUSSION

As observed in the SEM images, greater macrophage adhesion and activation occurs on Ti samples not coated in chitosan. However images of the chitosan-covered foil and chitosan-coated nanotube samples suggest that the nanotubes promote chitosan adherence, and thus have a lower amount of macrophage adherence and activation due to increased hydrogel attachment. This hypothesis was substantiated by florescence imaging, which revealed a smaller macrophage presence on chitosan-covered TiO_2 nanotubes than on any other sample. These initial results demonstrated that the chitosan-Ti anti-inflammatory system was successful in reducing macrophage activity. The addition of anti-inflammatory drug loaded nanoparticles with a 7 day release could further reduce the macrophage activation. Therefore, this system may have the potential to increase the amount of time the biosensor can remain *in vivo* before fibrotic encapsulation.

REFERENCES

[1] N. Wisniewski, M. Reichert, "Methods for reducing biosensor membrane biofouling," Colloids and Surfaces B: Biointerfaces, vol. 18(3), pp. 197-219. 2000.

[2] D. Higgins, et al. "Localized immunosuppressive environment in the foreign body response to implanted biomaterials," American Journal of Pathology, vol. 175(1), pp. 161-170. 2009.

[3] E. Yoo, S. Lee, "Glucose biosensors: an overview of use in clinical practice," in Sensors, vol. 10, pp. 4558-4576, 2010.

[4] S. Leibovich, R. Ross, "The role of the macrophage in wound repair. A study with hydrocortisone and antimacrophage serum," The American Journal of Pathology, vol. 78(1), pp. 71-100, 1975.

[5] T. Butterfield, et al, "The dual roles of neutrophils and macrophages in inflammation: A critical balance between tissue damage and repair," Journal of Athletic Training, vol. 41(4), pp. 457-465. 2006.

[6] L. Chamberlain, et al."Macrophage inflammatory response to TiO_2 nanotube surfaces," Journal of Biomaterials and Nanobiotechnology, vol. 2(3), pp. 293, 2011.

[7] V. Chenna, et al. "A Polymeric Nanoparticle encapsulated Small-Molecule Inhibitot of Hedgehog Signaling (NanoHHI) Bypasses Secondary Mutational Resistance to Smoothened Antagonists," Mol Cancer Ther, vol. 11, pp. 165-173. 2011.

1.0 Introduction

The use of biomaterials in applications such as prostheses, medical devices, and biosensors for treatment and diagnostics has become an important part of modern medicine. However, biomaterials used for human applications stimulate a negative immune response when implanted into living tissue. (Wisniewski, 2009) Inflammation is the first and most common response from the body once the presence of a foreign material is detected. (Wisniewski, 2009) In most cases this inflammatory response will lead to the formation of fibrotic tissue. In the case of biosensors, this tissue accumulation will ultimately result in device failure. (Higgins, 2009) For this Major Qualifying Project (MQP) team intends to design a system to reduce the inflammatory response that follows biosensor implantation, and to prevent fibrotic tissue formation. In performing these functions the device will extend the functional lifetime of implanted biosensors.

2.0 Literature Review

In order to create an anti-inflammatory system for a subcutaneous biosensor, some topics must be addressed so as to fully understand the scope of the project. Therefore, the factors of the immune system, biosensors, and previous solutions must be discussed. A review of biosensors will first be presented.

2.1 Biosensors and Inflammation

Biosensors have become a commonly used medical device, necessary for patients with a variety of disorders, but are largely associated with diabetes. To get accurate, constant readings of metabolites, the sensor must be implanted into the patient; various types of biosensors will be implanted into a patient. These sensors are used in a wide variety of applications, from glucose monitoring to examining the electrical impulses being sent from the brain. Depending upon the function of the sensor dictates the placement of the biosensor. (Yoo, 2010) This paper will be focusing on subcutaneous metabolite biosensors.

2.1.1 Biosensors

Metabolite biosensors are able to detect a wide range of analytes, including glucose and various amino acids. Patients will have a biosensor implanted into their skin and have it remain in a subcutaneous region for about one week before it must be replaced. The sensor will give accurate and constant readings on the patient's metabolite levels throughout the day, which can help in detecting fluxes and the daily patterns. (Vaddiraju, 2010) The sensor can either work on its own to report readings or can be synced with a drug delivery system for used in diabetic patients in the attempt to regulate the glucose concentrations before they reach critical levels. (Yoo, 2010) In order for these functions to be met, the biosensor needs to be sensitive to the surrounding environment, have a low response time, and be selective to the metabolites needing measurement so as to not generate results based upon other analytes. (Atta, 2011)
Back in 2004, the main form of biosensor was the glucose monitor, which accounted for about 85% of the $5 billion biosensor market. With the rise in diabetes and increased abilities and applications of biosensors, this market was expected to have doubled since then, therefore having a market value of around $10 billion. (Yoo, 2010)

Depending upon the necessary function of the biosensor dictates its location. In regards to metabolic, subcutaneous biosensors, the sensor is typically implanted in the abdomen region under the dermal skin layer. Therefore, the sensor is being inserted into the body at a depth between 4 and 12 mm. Depending upon the shape of the sensor, it can be inserted directly into the body, which causes torsional stress upon the sensor. The sensor can also be surgically implanted, where an incision is made in the skin prior to biosensor insertion, reducing the stresses exerted on the sensor.

In order to function properly, a biosensor needs to have the following key parts. It must have an electrode that can be implanted into the body, which in the third-generation glucose monitors is a needle-like projection. However, the electrode can also be a blunt-surfaced insert with a diameter of about 3 mm. The needle-like electrodes allow for a smaller puncture and easier insertion. The working and reference electrodes are what come into contact with the ions and metabolites in the interstitial fluid found in the body's subcutaneous region. (Yoo, 2010) The electrode pair is connected to an *ex vivo* segment where the metabolite levels are read and recorded every five minutes. Fig. 1 shows the components of the implantable section of a subcutaneous biosensor.
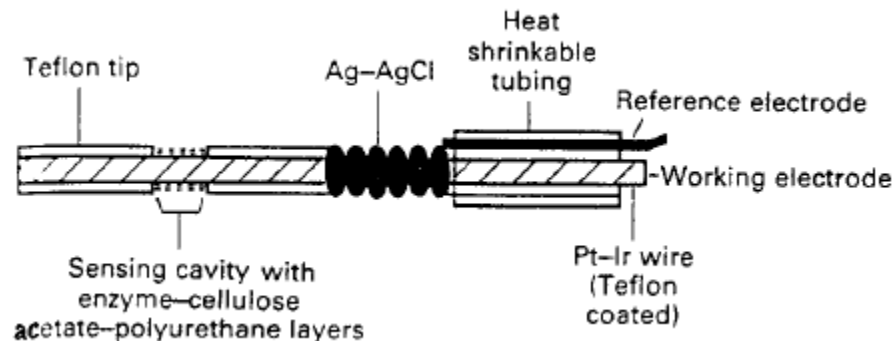
Figure 1: Diagram of a needle-like electrode of a subcutaneous biosensor (Wang, 2001)

The implantable segment is coated in bioinert materials to reduce the negative responses the body is capable of and to keep from exposing possible toxins to the region. Though this coating does still elicit an inflammatory response, the sensor is still able to function continuously for three to seven days. (Wang, 2001) However, after this time, the sensor must be removed due to the worsening inflammatory response.

2.1.2 Inflammatory Response
The human body's initial inflammatory response to the implantation of a biosensor is activated by the ensuing injury to vascularized connective tissue. The biosensor site responds to this insertion as it does any other wound, in three stages. These stages in include: acute inflammation, chronic inflammation, and tissue granulation.

2.1.2.1 Stage 1: Acute
Acute inflammation is a rapid response to tissue injury that can last anywhere from minutes to days. It involves exudations of fluid and plasma proteins similar to edema, including emigration of leukocytes, neutrophils and white cells that have moved from blood vessels to the perivascular tissue at the implant site. Neutrophils and monocytes accumulation is an important sign of the inflammatory reaction. (Anderson, 2001) This accumulates through adhesion, phagocytosis, and extracellular release of leukocytes. Following the release of leukocytes to the implant site, phagocytosis and release of enzymes due to activation of neutrophils and macrophages, degradation of biomaterial could possibly occur

depending on its properties. Some of the visual characteristic that the host experiences are: redness, heat, pain, swelling, and loss of function. (ProSono, 2006)

2.1.2.2 Stage 2: Chronic

The continuation of acute inflammation brings the inflammatory response to its second stage: chronic inflammation. (ProSono, 2006) One of the main characteristics of the chronic inflammatory response is the presence of macrophages, monocytes, and lymphocytes, with proliferation of blood vessels and connective tissue. The most important cell of the chronic inflammation is the macrophage since it produces a great number of biological active products. Some of these products are reactive oxygen metabolites, coagulation factors, and growth-promoting factors. These growth factors are involved in various stages of the wound healing response. (Anderson, 2001)

2.1.2.3 Stage 3: Tissue Granulation

Tissue granulation occurs after chronic inflammation has set in around the wound site. Granulation tissue can be describe as a pink, soft granular appearance on the surface of healing wound, and its ability to proliferate new small blood vessels and fibroblast. The primary tissue issues involved in this response is type I collagen which it predominates and help the formation of fibrous capsule. (Anderson, 2001)

2.1.3 Impact of Fibrotic Encapsulation

The immune system response described above that is generated by biosensor implantation is detrimental to the long term functionality of the sensor. The acute inflammation described in Section 2.1.2.1 is initiated immediately following the *in vivo* insertion of the biosensor, and a host of cells begin to accumulate at the site. The sensor is identified as a foreign body by the immune system, and as such the innate reaction is to phagocytize it to be either destroyed or presented to the T cells. This method is ineffective against a permanent structure such as a biosensor, and as such instead of being performed and reaching a natural conclusion the immune system continues to generate an inflammatory response. Although the continuous attack of the immune system upon the biosensor is unable to remove the device from the body, it does have a detrimental effect on upon both its structural integrity and ability to sense and diffuse analytes. (Wisniewski, 2009) The primary reasons for this loss of function, and eventual failure, include: electrical failure, delamination of membranes, enzyme degradation, membrane biodegradation, electrode passivation, fibrous encapsulation, and membrane bio-fouling. Fig. 2 depicts where on the biosensor these processes have an effect.
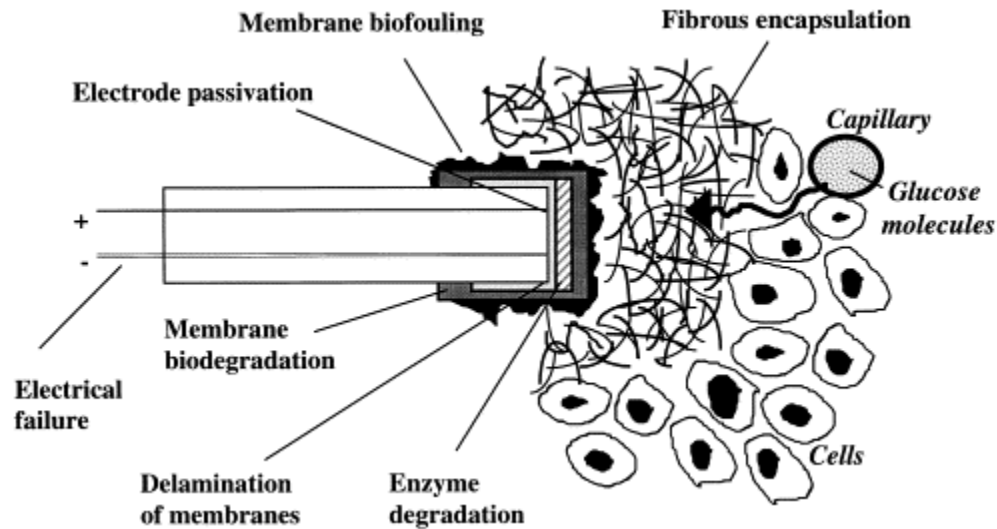
Figure 2: Schematic of Subcutaneous Biosensor Following Insertion (Wisniewski, 2009)

Although it has not been clinically determined which of these impediments poses the greatest restriction on biosensor longevity, fibrous encapsulation is the final effect of the inflammatory response and is ultimately the occurrence which halts device functionality. (Wisniewski, 2009) At the onset of acute inflammation, proteins and cells adhere to the surface of the biosensor to begin the process of membrane bio-fouling. Over an extended duration of time this deposition of proteins builds away from the membrane and forms a matrix that surrounds the biosensor. This matrix will impede the capabilities of the biosensor by blocking the signal interaction between the biological element and transducer. Once the capsule has reached a thickness of 500 micrometers, signal interaction is no longer possible, and the biosensor is no longer functional.

Though the biosensor was designed to be implanted in the body, long-term implantation has been a problem. As with all foreign implants, the body produces an immune response to counter the new material. In other types of implants, such as catheters, the immune response is not a big problem, but that is not the case with biosensors. The subsequent scar tissue capsule formation around the electrode impedes the ability for the metabolites to reach the biosensor. The initial impedance will lead to readings being different from the actual metabolite levels, but as the scar formation continues the biosensor eventually is unable to receive any readings. Even though the electrode is typically coated in a bio-inert material, the acute immune response will still be triggered. The term bio-inert refers to the fact that the material does not release toxins in the body or produce other negative effects. However, the formation of the scar tissue is what makes the material completely bio-inert as it will no longer be able to interact with the body whatsoever.

2.2 Current Anti-Inflammatory Approaches

Biosensors have a limited functionality due to the inflammatory response it elicits. In order to attempt to reduce this inflammation or otherwise ensure that the biosensor functions properly, there are a few currently used methods patients and doctors will employ. These current mitigations include frequent removal, addition of coatings, and drug delivery systems.

4

2.2.1 Biosensor Removal

Currently, a biosensor is only supposed to remain in the body for 3 to 7 days before being removed, replaced, and relocated. This is to ensure that the biosensor is fully capable of accurate and precise readings of the metabolites. If the biosensor stays in longer than the recommended time, the scar tissue formation will impede the metabolites ability to reach the biosensor, resulting in a failure of proper function. Therefore, the sensor is removed from that area and moved to another location. This process is repeated one or two times a week though it is painful, burdening, and expensive for the patients. (Yoo, 2010) It is because of this that there has been research looking into ways to increase the amount of time between sensor relocation.

2.2.2 Coatings

In the attempt to extend the life of the biosensor is to coat the implantable section of the electrode with a bio-inert material. This is typically a synthetic or a natural polymer that will not degrade or release any sort of toxin into the body. These materials do not produce a highly aggressive response and will not harm the body as it is not an excessive threat. (Oliveira, 2005) Commonly used synthetic coatings include Teflon, PEO, and PEG. (Yoo, 2010) Natural polymer coatings include alginate and chitin. (Wang, 2007) The coating must be carefully chosen and applied so as not to create an impenetrable barrier between the electrodes of the biosensor and the metabolites it monitors. If the coating proved to inhibit the biosensors function, then it is not worth the benefits of a reduced inflammatory response.

These coatings may help to deter the immune response for a short amount of time as it is not as large of a threat to the body as other materials, but it will still invoke the inflammatory response needed for healing the site. Because of this, the coating is many times used in addition to a drug delivery system, where the coating can help to secure the delivery vehicles to the biosensor to prevent migration. (Vaddiraju, 2010)

2.2.3 Drug Delivery

Another method of prolonging biosensor functionality is the delivery of anti-inflammatory drugs into the areas of biosensor insertion. A common drug used for this is dexamethasone, which is quite effective in reducing inflammation and does not have extensive side effects when delivered locally. Many studies have been conducted utilizing different delivery methods for dexamethasone and other anti-inflammatory drugs. Injection is a delivery possibility, though it is limited as it allows for spikes in the amount of drug injected, but does not regulate a controlled, continuous release. In order to attain this more continuous release as opposed to temporary spikes, microspheres, nanotubes, and degradable coatings have been used. The microspheres and degradable coatings are made of degradable or porous polymers that contain the anti-inflammatory drug. For degradable polymers, the rate of the degradation dictates the rate at which the drug is released. In the porous polymers, the rate of dispersion depends upon the pore size and the environmental factors effect on the rate of diffusion. The polymers that make up these coatings and microspheres are typically PGLA, which is used for its bio-inert characteristics and well-defined degradation rate. (Jayant, 2007) However, for a natural microsphere, alginate is commonly used. (Wang, 2007) Nanotubes are another form of drug delivery which utilizes diffusion to release the drugs into the body. The nanotubes are typically made of carbon and vary in size depending upon the duration of drug delivery needed. They are typically put in a bio-inert coating to keep them close to the insertion site and reduce the possible migration.

3.0 Project Strategy

To begin the design process for this project, a client statement was composed to meet both client needs and the problem of inflammatory impediments to biosensor functionality. Design objectives were developed from that statement, as well as design constraints. Certain constraints were a result of the Worcester Polytechnic Institute (WPI) MQP structure, and while they were considered it was acknowledged that they are not unique to this problem.

3.1 Client Statement

Professor Anjana Jain of WPI's Biomedical Engineering (BME) Department commissioned the team to design an anti-inflammatory device that could be used in conjunction with an *in vivo* biosensor to reduce initial inflammation at the site of biosensor insertion, delay development of fibrotic scarring, and ultimately extend the functional lifetime of that biosensor. Additional objectives included developing a device that is cell specific, localized in its effect, operational immediately following insertion, and is easy to apply to the biosensor. As it is to be used *in vivo*, the device must also be biocompatible.

3.2 Objectives

The following is a ranked list of design objectives generated from the client statement and correspondence with the advisor.

- Biocompatible
- Compatible with Biosensor Operation
- Long Lasting
- Localized
- Immediate
- Cell Specific
- Easy to Apply

The two primary objectives identified by the team are that the device be biocompatible and compatible with biosensor operation. The former is fairly obvious in its importance; if the anti-inflammatory device is not compatible with the human body then it will produce more of an immune response then the sensor itself and could be rejected outright. The latter, that the device be compatible with biosensor operation, is to ensure that whatever anti-inflammation method is utilized has neither a negative physical effect on the biosensor nor a negative effect on the sensor's functionality. These objectives were ranked to be of the highest priority because should they not be met it is unlikely that any successful outcome will result. "Long Lasting" was ranked third as an objective as the ultimate goal of the device is to extend the functional lifespan of the biosensor. In order to do so the device must be long lasting itself or its effect must be. Localized, immediate, cell specific, all refer to the effect of the anti-inflammatory device, and were determined to be important but not crucial to the success of the device. It is preferable that the three objectives be met, but the team can envision working scenarios where one or more are not. The objective "easy to apply" was ranked the lowest of all seven. It refers to the ability of the user to apply the device to either the patient or the biosensor, an ability that would have an effect during testing and on marketability

3.3 Constraints

Below is a list of design constraints exclusive to this MQP:

- All materials must be biocompatible
- Lack of human immune system on which to test
- System must not impede biosensor function
- System must not permanently affect the immune system

Additional constraints ubiquitous to all BME MQP projects:

- Budget
- Development and testing time
- Limits on material selection and availability
- Follows regulatory requirements and is safe for user and patient

The initial four constraints listed are specific to this MQP and its device. Firstly, as the device must be biocompatible, as previously stated in section 3.1, there are severe limitations on what materials are available to use in the design. Anything that is toxic or produces a negative response in the body must be immediately disregarded. Secondly, although the team is designing a device to be used in the human body, there is no possibility that it could be tested in human patients. Therefore a model of the human immune system must be developed for testing, the limitations of which for a constraint on the design and testing process. That the system must not impede biosensor function is similar to the objective on biosensor compatibility and, like the biocompatibility constrain, imposes restrictions on the material, shape, and size of the device. Finally, the last constraint is that the system must not permanently affect the immune system. This constrain is not limited to a permanent negative effect, as a permanent neutral effect would be just as unwanted in a human subject.

The additional four constraints, listed separately, refer to limitations that all MQPs at WPI are bound by. There is a finite amount of money that is dedicated to the project, as well a definite duration of time. Materials are limited based on monetary reasons, and on the team and advisor's ability to obtain them. All projects and devices must be safe for the user and patients that they are intended for, and must comply with all federal and state regulations pertaining to their use.

4.0 Design Selection

Final design selection was made by gathering the information obtained from the literature review and analyzing how each potential option would meet the previously determined client statement, objectives, and constraints. The selection of final design components, how they are expected to work in conjunction with one another, and the rationale behind their selection is found below.

4.1 Macrophages

Macrophages are differentiated monocytes that participate in the innate immune system. They were selected as a design component as they are the primary phagocytic cells in inflammatory response, and immigrate to the site of injury from the surrounding blood vessels. Once present macrophages either engulf cellular debris and foreign bodies, or stimulate the action of lymphocytes, an immune cell involved in the second stage of the inflammatory response. (Leibovich, 1975) Therefore, by reducing macrophage activity around a biosensor it is possible to reduce the entire inflammatory response and thus delay the occurrence of fibrotic scarring.

4.1.1 Stage of Inflammation

Within hours after injury has occurred to the vascularized connective tissue macrophages begin to proliferate at the site. (Leibovich, 1975) At this stage local proteins have already begun to opsonize the identified foreign bodies, which allows for macrophages to adhere to and phagocytize these particles more easily. Macrophages will continue to diffuse into the wound site via diapedesis from nearby blood vessels throughout the entirety of the acute stage of inflammation, and will reach maximal concentration levels at roughly the third day following injury. (Leibovich, 1975) Although macrophages will reach peak numbers at this stage, they remain at the site for up to 16 days and thus carry into the second stage of inflammation. (Butterfield, 2006)

4.1.2 Location of Macrophages

Macrophages are present in small quantities in almost every tissue at all times. (Sorg, 1991) Once activated by tissue injury cells migrate en masse and adhere to the location site by diffusing through the blood vessels. In addition to performing phagocytosis, adhered and activated macrophages secrete pro-inflammatory cytokines that encourage the proliferation of additional macrophages to the location. (Butterfield, 2006) This generates a positive-feedback response that ensures the constant presence of the cells for as long as the inflammation process lasts.

4.1.3 Impact of Macrophages on Biosensor Implantation

Macrophages limit biosensor longevity by exacerbating the inflammation response caused by device insertion. The positive-feedback loop referenced in the previous section maintains a continuous immune response until the foreign particles are able to be phagocytized and removed which, in the case of biosensors, is impossible. As a result, activated macrophages continue to secrete inflammation-inducing cytokines that progress the inflammatory response from the acute stage to tissue granulation. Macrophage interactions with proteins can also prove to be detrimental to biosensor functionality. Proteins begin to coat the sensor surface immediately following implantation, which attracts macrophages. (Leibovich, 1975) As macrophages are unable to phagocytize the surface they gradually accumulate, and eventually form the inner layer of fibrotic scarring. Because of the primary role that macrophages play in the acute inflammatory response, and thus the ensuing fibrotic scarring, they were selected as the principal target of the anti-inflammatory system. Effectiveness of this system could then be determined by observing macrophage activity; specifically, the adhesion and activation of the macrophages to the foreign surface would indicate its biocompatibility and the level of the acute inflammatory response.

4.2 Titania Nanotubes

The high biocompatibility, among other favorable mechanical properties, of Titanium (Ti) has increased its viability in medical instruments and implants. As a result Ti and Ti-based alloys are commonly utilized in devices ranging from dental implants to fracture fixations, where strength, corrosion-resistance, and bioadhesion are necessary. (Doong, 2010) Titania (TiO_2) nanotubes, or anodized Ti foil, have been found to demonstrate increased levels of this inherent biocompatibility, for reasons which are yet unknown, particularly when in contact with macrophages. As described in Section 4.1, when introduced to a foreign material macrophages adhere to its surface and subsequently activate, recruiting more cells. However, interactions with TiO_2 nanotubes have shown a decrease in macrophage surface adhesion, as well as a reduction in the number of activated macrophages, when compared to a Ti foil control. (Chamberlain, 2011) (Rajyalakshmi, 2011) As a result of these studies, particularly the fact that the primary component

of the inflammatory response-macrophages-are affected, TiO_2 nanotubes were selected as a primary component and structural basis of the anti-inflammatory system design.

4.3 1% Chitosan Gel

Hydrogels have proven useful in a vast number of medical applications, being used as regeneration scaffolding, drug-delivery vehicles, and biocompatible coatings. It is the latter function that is of greatest interest in this design selection, as a hydrogel would have the ability to coat the TiO_2 foundation of the system and, ideally, increase its biocompatibility. The primary division between hydrogel types, and the determining factor in their medical application, is whether they are found naturally or are synthetically created. Synthetic hydrogels allow for consistency in results as they have been engineered to meet certain mechanical criterion. These synthetic hydrogels can be altered to remain for a long period of time in the body, have varied strength and elasticity, and even be altered *in vivo* depending upon the environment. In comparison, although natural hydrogels are more difficult to modify, they are more biocompatible; their natural state does not elicit the extreme inflammatory response that a synthetic polymer typically does. As biocompatibility is the most essential characteristic of components within this anti-inflammatory system, a natural hydrogel was selected for the design. Within the realm of natural hydrogels, there is a wide range of options. Polymers such as collagen are found naturally in the human body whereas chitosan, alginate, and other natural hydrogels are taken from other organisms, such as plants and crustaceans. Of these chitosan stands out as a non-toxic, biodegradable, non-immunogenic hydrogel that is a deacetylated form of chitin. It can be used in many different applications, such as viscous solutions, spray-dried powders, and nanoparticles, depending upon the exact needs of the project. A viscous solution of chitosan gel would be the most optimal in this case at it creates a natural hydrogel that can be applied to a biosensor while also housing anti-inflammatory drugs or drug-releasing nanoparticles. This application has been utilized in previous studies, demonstrating that the hydrogel coating will not impede the sensitivity of the biosensor. (Muzzarelli, 2000)

4.4 PLGA Nanoparticles

Poly (lactic go-glycolic acid) (PLGA) is a common synthetic hydrogel widely used in drug-delivery application. It has been proven to be biodegradable, biocompatible, and modifiable, making it very attractive for use in delivering anti-inflammatory drugs to the site of a biosensor implantation. Many other hydrogels have been utilized to make nanoparticles, such as alginate, poly(vinyl alcohol) (PVA) and poly(ethylene oxide) (PEO). Each of these nanoparticles differs in size, degradation time, and various mechanical properties. (Hamidi, 2008) PLGA has the benefit of degrading into biocompatible compounds, lactic acid and glycolic acid, which are non-toxic to the human body. During the formation of these nanoparticles, the ratio of lactic acid and glycolic acid as well as the molecular weight dictates the degradation rate, allowing the particles to remain present and deliver drugs anywhere from weeks to years. For this project a degradation time of a few weeks was desired in order to avoid potential toxicity, and to be able to quantify the release profile in the limited amount of testing time (Danhier, 2012) A PLGA nanoparticle concentration of 12.5mg/mL was therefore selected to be imbedded in the chitosan hydrogel and increase the viability of the anti-inflammatory system.

4.5 Anti-Inflammatory System

In order to create an anti-inflammatory system that would prevent the development of fibrotic scarring and extend the functional life of a biosensor beyond the current 3 to 7 days the TiO_2 nanotubes are to be

used in conjunction with 1% chitosan hydrogel, and PLGA nanoparticles. Ultimately, the biosensor itself would be made of Ti and anodized to create TiO$_2$ nanotubes. This biosensor would then be dip-coated with PLGA nanoparticle-loaded chitosan hydrogel, as illustrated in Fig. 3.
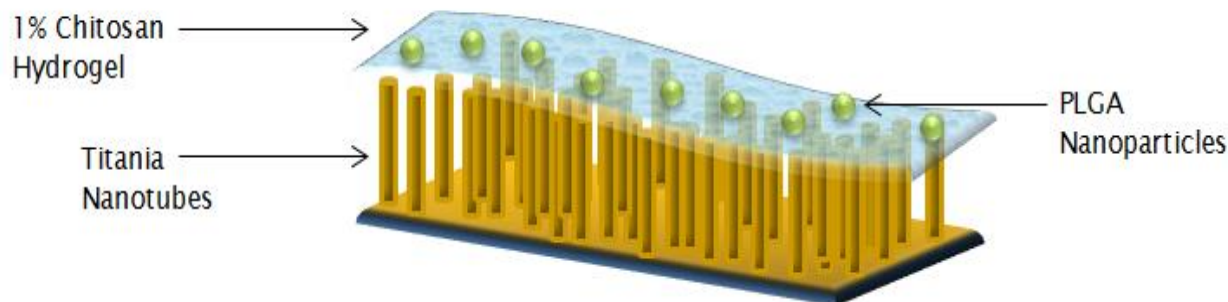
Figure 3: Schematic of complete anti-inflammatory system

The PLGA nanoparticles would be embedded with dexamethasone, providing a more general reduction in the inflammation in addition to the macrophage-targeting nanotubes and biocompatibility-increasing hydrogel. It was hypothesized hypothesis that this system could reduce inflammation by synergistically preventing macrophage activation and reducing the overall cell response to the presence of a foreign body, subsequently preventing fibrotic scarring and increasing biosensor longevity. The following methods were utilized for the creation of the components of this system.

5.0 Methodology

In order to create this anti-inflammatory system for a subcutaneous biosensor, each component required creation and testing. Those components are the TiO$_2$ nanotubes, the chitosan hydrogel, and the anti-inflammatory drug-loaded PLGA nanoparticles. After these components are created and tested, they can be combined to create the final system.

5.1 Titanium Nanotubes

TiO$_2$ nanotubes are formed by anodizing Ti foil, the depiction of which can be found in Fig. 4. In this study, Ti foil (99% pure, 0.127mm thick) was cut into 3x5 cm pieces and ultrasonically cleaned in 100% isopropanol for 15 minutes. Samples were anodized at 15V in 0.25M hydrofluoric acid for 45 minutes and subsequently annealed in a tube furnace at 400°C for 4 hours. After annealing, Ti samples were rinsed with DI water, pure isopropanol, and ultrasonically cleaned in pure isopropanol for 15 minutes. Scanning electron microscopy (SEM) imaging was used to characterize the annealed samples. The complete list of materials and protocol for this procedure can be found in Appendix A.
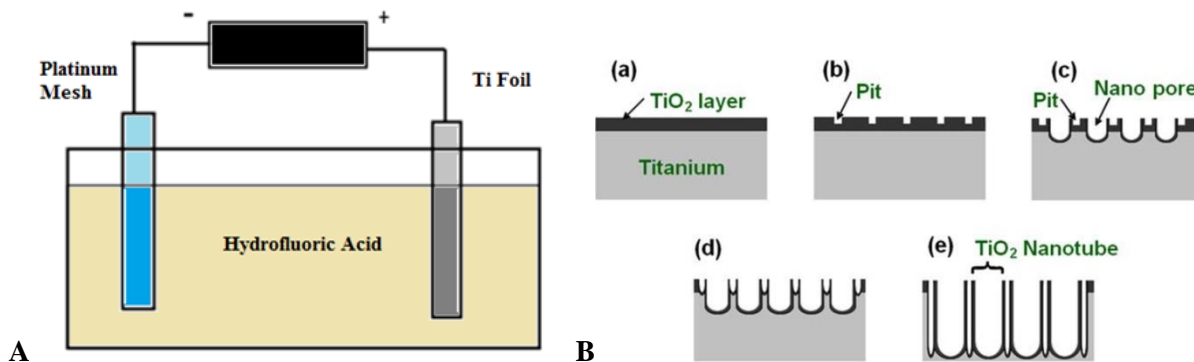
Figure 4: (A) Depiction of anodizing system with Platinum mesh anode and Ti foil cathode, (B) Schematic nanotube formation during anodization (Brammer, 2011)

In order to determine the size of the nanotubes, ImageJ software was utilized. The Image J measuring tools were calibrated and scaled to match the 400nm scale bar on the SEM images obtained during earlier characterization. Examples of these SEM images can be found below in Fig. 5. The inner and outer diameters of the tubes were measured , with the diameters were taken from the widest and narrowest sections and then averaged together. Approximately 70 nanotubes, which accounted for over 80% of the tubes on each image and roughly 134 values, were measured and averaged in order to get a proper representation of the tubes imaged. The data from this analysis is included in Appendix B. Prior to all *in vitro* testing TiO$_2$ samples were cut into 0.5x0.5 cm squares and ultrasonically cleaned in pure ethanol in order to ensure sterility.
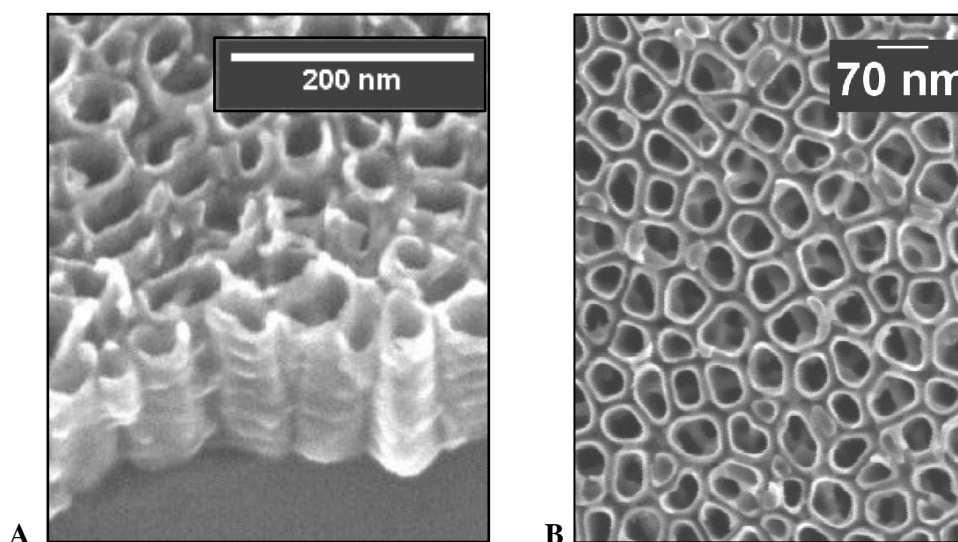
Figure 5: (A) Side view of annealed TiO$_2$ Nanotubes, (B)Top-down cross section of annealed TiO$_2$ Nanotubes

5.2 1% Chitosan Gel

Chitosan from Sigma (from shrimp shells, ≥75% deacetylated) was dissolved in 2% acetic acid solution by magnetic stirring for 2 hours. The gel was then stored at room temperature until testing. For further information refer to the complete protocol in Appendix C. TiO$_2$ and Ti samples were dipped in the gel prior to *in vitro* testing, and placed into individual wells in a 48-well plate. The coated samples in coated samples were then refrigerated at 4°C for 24 hours to dry, and then placed in a 37°C oven until testing.

This final step was performed to ensure that the dried gel would not change in consistency when introduced to incubation temperatures. As no change was observed in the gel when transferred from the refrigerator to the oven, no further testing was performed on the chi-coated samples prior to cell seeding.

5.3 PLGA Nanoparticles

PLGA nanoparticles have the ability to maintain a sustained drug release profile for an average of 2 weeks. For this delivery system, the anti-inflammatory drug dexamethasone would be utilized. However, in order to allow for ease of testing, FITC was used as it has a comparable molecular weight to dexamethasone, 389.38 g/mol versus 392.46 g/mol respectively. FITC has fluorescence which will enable the release to be very easily quantified. The FITC was therefore loaded into the PLGA nanoparticles in the following procedure.

5.3.1 Nanoparticle Fabrication

In order to create the PLGA nanoparticles, a 5050 DLG mPEG 5000 (PLGA-PEG) was obtained from Evonik Corporation and utilized. These nanoparticles were created by dissolving 50 mg of the PLGA-PEG mixture with 1 mg of FITC into a round bottom flask containing 400 μL of dichloromethane and 100 μL of acetone. After the powders had completely dissolved, 2.5 mL of 4% polyvinyl alcohol (PVA) was added. This mixture was then sonicated for 3 minutes at a strength of 20W while being kept on ice. After sonification, the solution was rotor-evaporated until there had been a complete evaporation of the organic solvents. The remaining solute was resuspended in 3mL of ultrapure water. This suspension was then ultracentrifuged at 40,000 rpm for 45 minutes. The resulting precipitated nanoparticle pellet was then washed three times with ultrapure water. The pellet was resuspended in 3mL of ultrapure water and underwent mild sonication. This was centrifuged at 3,000 rpm for 5 minutes in order to remove any large aggregates. The solution was then flash-frozen on dry ice and lyophilized. In order to use the particles in further testing, they were resuspended in ultrapure water. The protocol for this process is included in Appendix D. The nanoparticle size was determined using Dynamic Light Scattering (DLS). As seen in Fig. 6, the nanoparticles had an average diameter of 170 nm.

		Diam. (nm)	% Intensity	Width (nm)
Z-Average (d.nm): 170.3	Peak 1:	220.8	92.8	102.4
PdI: 0.277	Peak 2:	36.59	5.0	9.819
Intercept: 0.941	Peak 3:	4942	2.1	642.6
Result quality : Good				
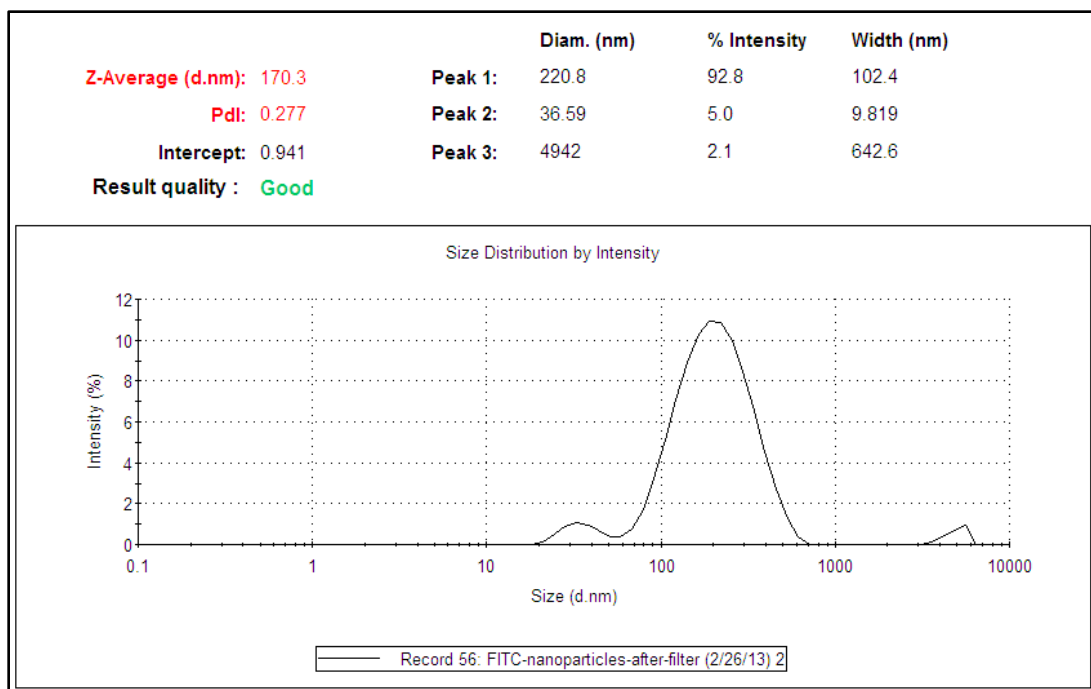
Figure 6: DLS Graph displaying average diameter of FITC loaded PLGA nanoparticles

5.3.2 FITC Release Study

A standard curve for Fluorescein isothiocyanate (FITC) was prepared using concentrations of 0.5 μg/mL to 350 μg/mL FITC in PBS.

To begin the study, the nanoparticles were re-suspended in PBS to create a 25 mg/mL solution. This solution was then mixed in a 1:1 ration with warm, liquid 2% agarose gel to create a 12.5 mg/mL nanoparticle solution which yields a 2% FITC concentration. Three capped, glass vials (vials 1-3) were filled with 100 μL of this agarose/nanoparticle solution and refrigerated to solidify the solution. Another three vials (vials A-C) were each filled with 150 μL of the solution and also refrigerated. After the gel had fully solidified (about 10 minutes after refrigeration), PBS was added to each vial, 250 μL in vials 1-3, and 300 μL in vials A-C. The vials were left for 24 hours in 37°C to simulate *in vivo* conditions. After 24 hours, the PBS from each vial was collected and put into separate vials, then frozen. The PBS was replaced in each vial to equal the amount taken out. This process was repeated with time points at 1, 2, 3, 5, 7, 9, 11, and 13 days. A protocol of this process is included in Appendix E. At the end of harvesting, the concentrations were analyzed with a Thermo Scientific Nanodrop 2000 Spectrophotometer in order to find the absorbance of the FITC to be compared to the standard curve.

5.4 In Vitro Testing: Macrophage Viability, Adhesion and Activation

The adhesion and activation properties of macrophages dictate the body's immune response to a foreign material. As macrophage activation produces a different morphology than that of an inactivated cell, as seen in Fig. 7, qualitative data generated through images of the cells adherence to the different samples can indicate the intensity of the immune response. The samples to be tested for activation were an unmodified Ti foil control, TIO_2 nanotubes, chitosan-coated Ti foil, and chitosan-coated TIO_2 nanotubes.
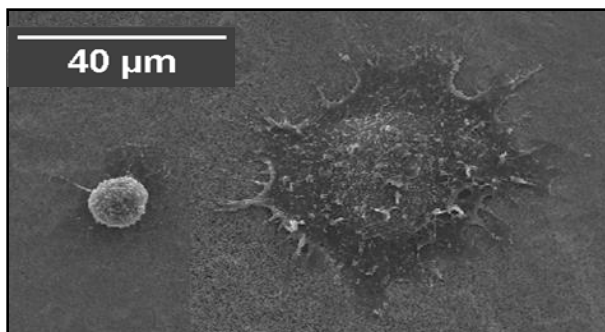
5.4.1 Macrophage-like Cells

Immortalized macrophage cells, which consisted of macrophages harvested from C57bl/6 mice and treated with J2 virus in order to enable proliferation, were obtained as a gift from University of Massachusetts (UMASS) Medical School in order to gather preliminary adhesion and viability data. A media mixture of DMEM, 10% FCS, HEPES (11 ml of 1M per 500 ml bottle), and Cipro was used throughout for these immortalized macrophages. 10,000 cells were seeded per well, with each column of the well plate containing Ti foil controls, TIO$_2$ nanotubes, chitosan-coated Ti foil, or chitosan-coated TIO$_2$ nanotubes; a schematic of this procedure can be found below in Fig. 8.
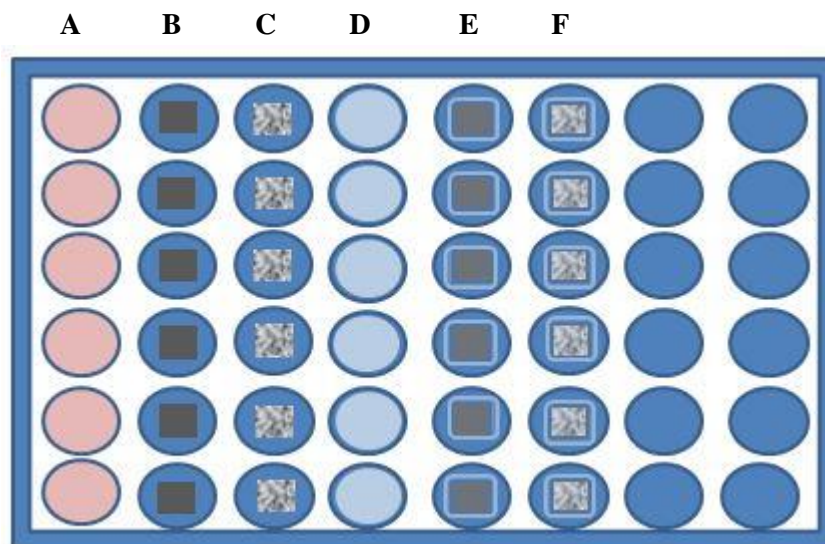
Figure 8: Schematic of 48-well plate containing (A) media control, (B) Ti foil control, (C) TiO$_2$ nanotubes, (D) Chitosan, (E) Chitosan-coated Ti foil , and (F) Chitosan-coated TiO$_2$ nanotubes

Two well plates containing identical substrates were utilized; one was allowed to proliferate for 24 hours and the other for 7 days. These durations were chosen because of their correspondence to the inflammatory response: 24 hours is the period during which initial macrophage activity would occur, and 7 days is the desired period of time to extend biosensor functionality. Due to the ability of the immortalized macrophages to proliferate accurate viability, adhesion, and activation data were difficult to obtain. Therefore all initial testing using these cells was performed solely to validate experimental concepts and testing procedures.

5.4.2 Macrophages

To rectify the problem of macrophage proliferation, primary macrophages from C57 Black /6J (C57BL/6J) mice were obtained as a gift from UMASS Medical School. The above procedures were duplicated using this cell line, substituting the previous media for DMEM supplemented with 10% Fetal Bovine Serum and 1% Penicillin/Streptomycin. Following either 24 hours or 7 days, depending on the well plate, substrate samples were stained to determine macrophage viability and adhesion, and imaged to determine macrophage activation.

5.4.2.1 Hoechst and Phalloidin Staining

To determine macrophage viability and adhesion, a Hoechst and a Phalloidin stain were used on half of the samples in each well plate. The Phalloidin, which stains the F-actin filaments green, was prepared by mixing 5 μL of stock Phalloidin with 200 μL of PBS TWEEN, resulting in a dilute solution. The Hoechst stain, which stains cell nuclei blue, was prepared by mixing 1 μL of stock Hoechst with 1000 μL of PBS TWEEN, resulting in a usable dilute solution. To begin the study, the cells were washed twice with 10% PBS, and then fixed in 2% formaldehyde for 60 minutes. The wells were then washed three times with PBS. After aspirating the PBS, 2% BSA blocking agent was added to each sample and left for 5 minutes before being aspirated out. The dilute Phalloidin solution was added to each sample and left for 15 minutes, making sure the sample was submerged. After, the Phalloidin solution was aspirated out and the dilute Hoechst solution was added to each well, enough to cover the sample, and left for 5 minutes. The stain solution was then aspirated out of the wells and replaced by 10% PBS, then stored in the 4°C fridge until imaging. A protocol of this procedure can be found in Appendix F. The samples were kept out of light by being wrapped in aluminum foil upon storage. A Leica Fluorescent Microscope system with image analysis software was used to image and record the samples.

5.4.2.2 SEM Imaging

SEM was utilized to qualitatively assess the adhesion and activation of the macrophages. The remaining half of the Ti and TiO2 samples in each well plate, those not used in staining, were imaged obtain these data. In order to prepare the samples for imaging, the cells first had to be fixed. This was done by adding approximately 4 μL of 2.5% gluteraldehyde to each media-filled well. After 10 minutes, the gluteraldehyde and media was aspirated out and another 5 μL of 2.5% gluteraldehyde was added to each well, ensuring the sample was covered. The sample was left in the gluteraldehyde for 15 minutes, and then the solution was aspirated out. A series of alcohol washes was then performed. First, 10% alcohol was added dropwise to each well until the sample was covered (approximately 5 drops) and then left for 10 minutes. The alcohol was then aspirated out and this procedure was repeated using 30%, 50%, 70%, 85%, 95%, and 100% ethanol. The samples were not allowed to dry out, so well by well, the ethanol was aspirated and immediately the higher concentration was added. After the 100% ethanol, each well was washed once more with the 100% ethanol. The cell fixation protocol can be found in Appendix G. The samples were then point-dried using an AutoSamdri-815 critical point dryer at UMASS Medical School. After all of the samples had been point dried, they were sputter-coated with 12 nm of gold/palladium alloy in a Cressington 208HR sputter coater at UMASS Medical School. An FEI Quanta 200 MKII FEG ESEM machine at UMASS Medical School equipped with an Oxford-Link EDS system was used to examine the sputtered samples. Images were taken of each of the samples for further analysis.

6.0 Results

Through the aforementioned methodology, qualitative data demonstrating a validation of design concepts and design ability to reduce macrophage activity were obtained. Results on TiO_2 nanotubes characterization and PLGA nanoparticle release were obtained separately from *in vitro* testing, which constituted the primary area of interest.

6.1 Titania Nanotubes

The TiO_2 nanotubes were imaged using SEM at Northeastern University. These images were then analyzed using ImageJ to determine the average inner and outer diameters of the tubes. It was determined that the average inner diameter of the nanotubes was 42.3 nm and the average outer diameter was 63.8 nm. This was slightly less than the suggested diameter of 70 nm. These tubes were also found to have an approximate length of 200 nm. SEM images of the TiO_2 nanotubes following *in vitro* were also taken, and will be discussed in Section 6.3.2.

6.2 FITC Release Study

The FITC release study from the PLGA nanoparticles lasted the full 13 days of the study. The collected supernatant had been stored in the fridge until all sampled had been collected. Using a Thermo Scientific Nanodrop 2000 Spectrophotometer, the absorbance of solutions was analyzed in Alexa Fluor 488 and taken in triplicate. Each day's readings were averaged together to get the mean and the standard deviation. These absorbance values were matched against the standard curve seen in Fig. 9. The equation of the linear-fit line was utilized in order to find the experimental FITC concentrations based upon the absorbance readings.
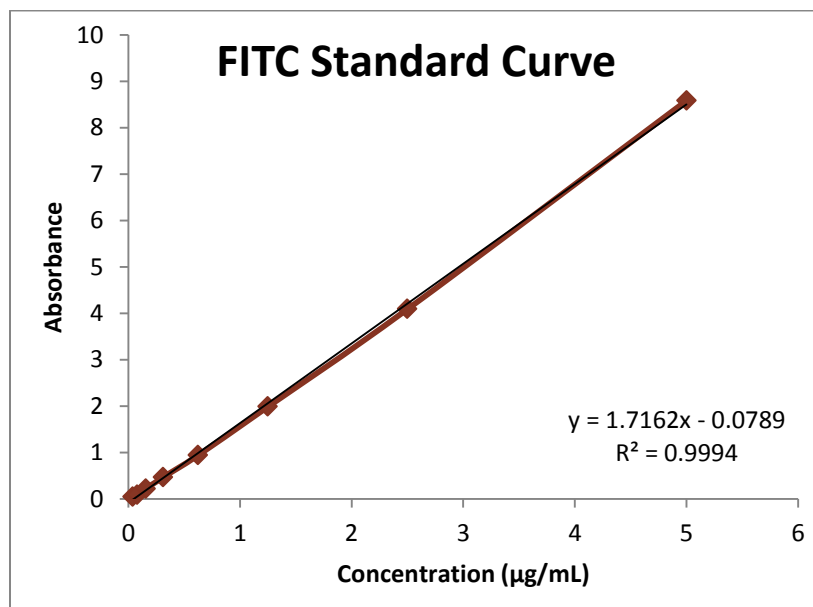
Figure 9: Standard curve of FITC absorbance vs. concentration with a slope of 1.7162 and a fit of 0.9994

Once the average absorbance was converted into average concentrations for each time point, they were plotted versus time in order to get the cumulative release curve found in Fig. 10. This was done for both the low volume wells of 100 μL of the 12.5 mg/mL nanoparticle/PBS solution and the high volume wells of 150 μL of the 12.5 mg/mL solution.
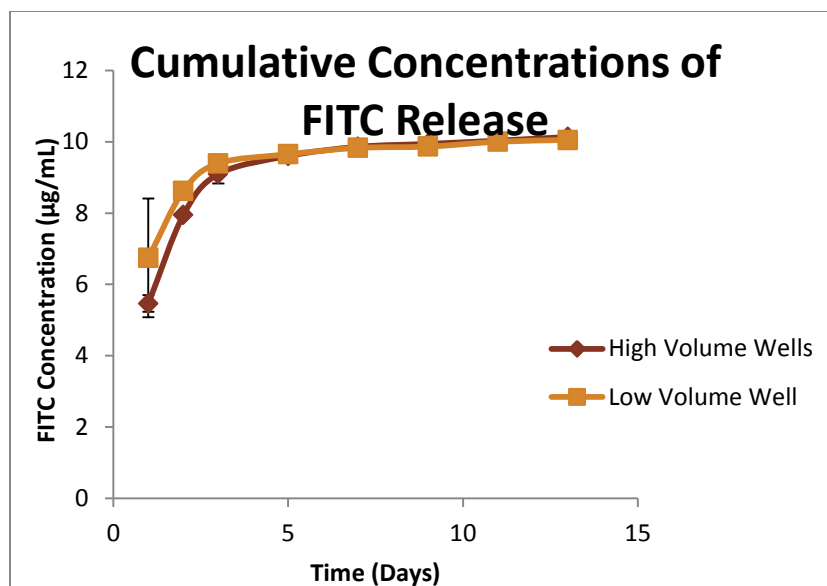
Figure 10: Cumulative concentration of FITC release from high volume and low volume wells demonstrating similar release profiles over the course of two weeks

The resulting curves had an initial burst for the first 48 hours, after which it began to level. From day 5 until the end of testing at day 13, the release remained quite constant at a concentration of 10 µg/mL.

6.3 In Vitro Testing:

The *in vitro* testing conducted on Ti foil, TiO_2 nanotubes, chitosan-coated Ti foil, and chitosan-coated TiO_2 nanotubes allowed the group to truly qualify the system design and determine if it was viable for future applications. The primary macrophages were utilized over the immortalized macrophages during this testing in order to gain an accurate assessment of cell viability without factoring in cell proliferation. During testing substrates were analyzed for macrophage viability, adhesion, and activation through Hoechst and Phalloidin staining and through SEM imaging.

6.3.1 Hoechst and Phalloidin Staining

Images of each sample were taken at the area of highest macrophage confluence, and both the green Phalloidin staining of the cell actin and blue Hoechst staining of the cell nuclei were apparent. Ti foil demonstrated higher rates of macrophage adhesion after 24 hours; however from observations of the location of cell action seen in Fig. 11 there did not appear to be any activation.

Figure 11: Fluorescence imaging of (A) Ti foil, (B) TiO$_2$ nanotubes, (C) Chitosan-covered Ti foil, and (D) Chitosan-covered) TiO$_2$ nanotubes after 24 hrs. Green Phalloidin is staining cell actin and blue Hoechst is staining cell nuclei

Both Ti foil and chitosan-covered Ti foil had increased amounts of macrophage adhesion and activation after 7 days in comparison to the TiO$_2$ and chitosan-coated TiO$_2$ nanotubes. TiO$_2$ and chitosan-coated TiO$_2$ nanotubes possessed equal amounts of cellular adhesion; however the macrophages on the chitosan-coated samples were less activated than on those without the hydrogel as evidenced by the Phalloidin stain in Fig. 12.
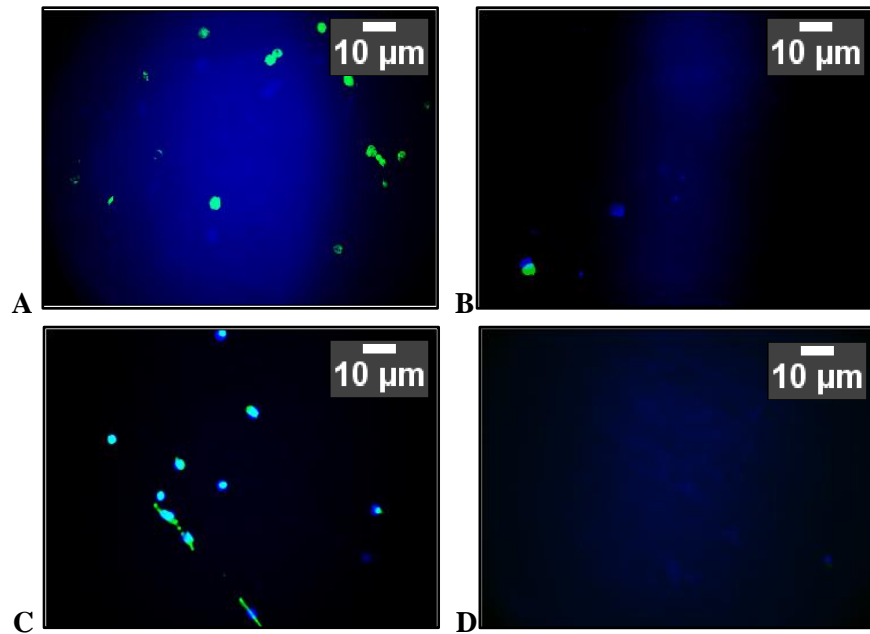

Figure 12: Fluorescence imaging of (A) Ti foil, (B) TiO$_2$ nanotubes, (C) Chitosan-covered Ti foil, and (D) Chitosan-covered TiO$_2$ nanotubes after 7 days. Green Phalloidin is staining cell actin and blue Hoechst is staining cell nuclei

6.3.2 SEM Imaging

All samples demonstrated an amount of macrophage adhesion and activation, which was determined by cell morphology as discussed in Section 5.4. Ti foil possessed the highest amount of adhesion and activation among the 24 hours samples; chitosan-coated samples possessed the least with nearly all of the adhered macrophages remaining inactivated. Fig. 13 below depicts differences in macrophage adhesion and activation between the four sample types after 24 hours.
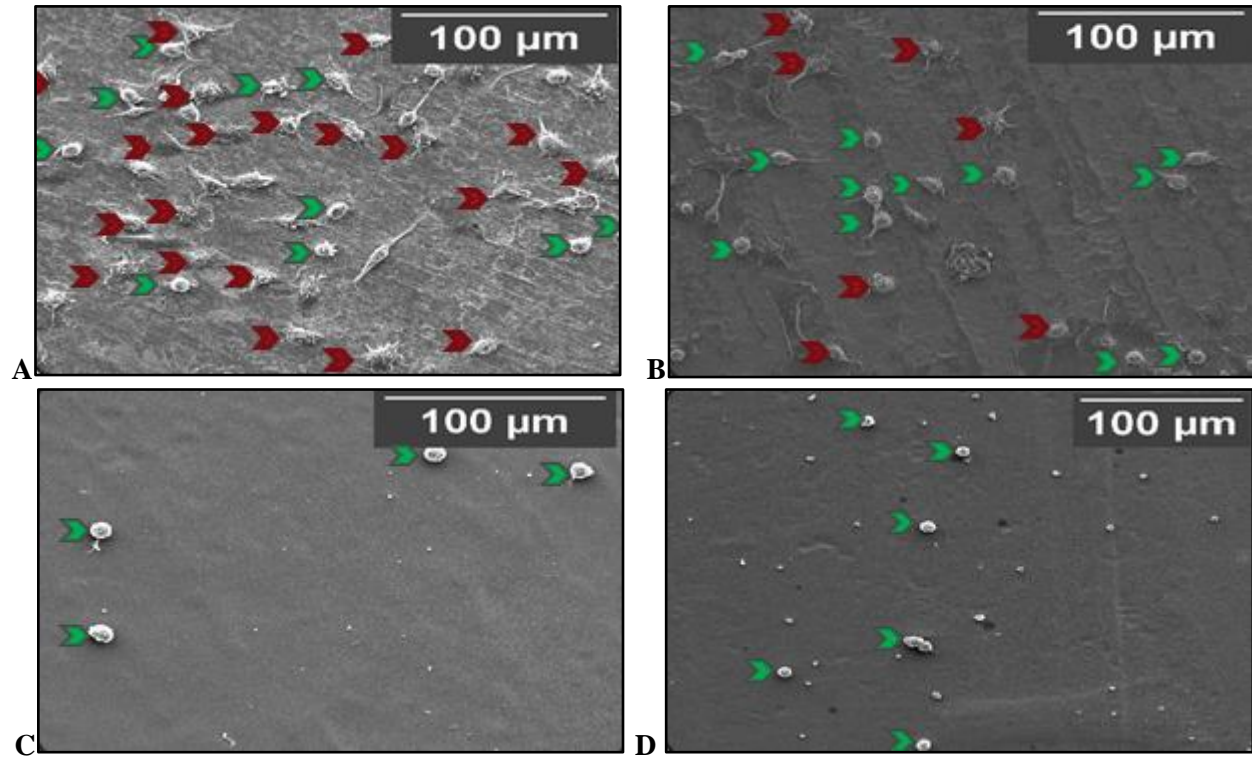
Figure 13: SEM images of (A) Ti foil, (B) TiO$_2$ nanotubes, (C) Chitosan-covered Ti foil, and (D) Chitosan-covered TiO$_2$ nanotubes 24 hrs after macrophage seeding. Green arrows indicate inactivated macrophages, red arrows indicated activated macrophages.

 After 7 days both the Ti foil and TiO$_2$ chitosan-coated samples demonstrated minimal adhesion and activation in comparison to the non-chitosan coated samples. SEM images of these samples are seen in Fig. 14. Areas where the chitosan layer had torn were more attractive to macrophage adhesion, as can be observed in in part C of Fig. 14.
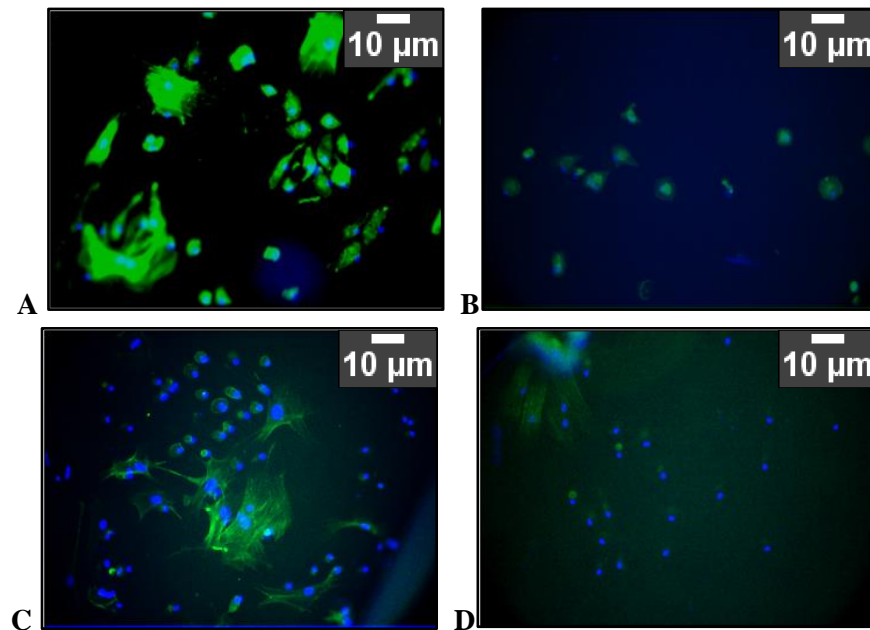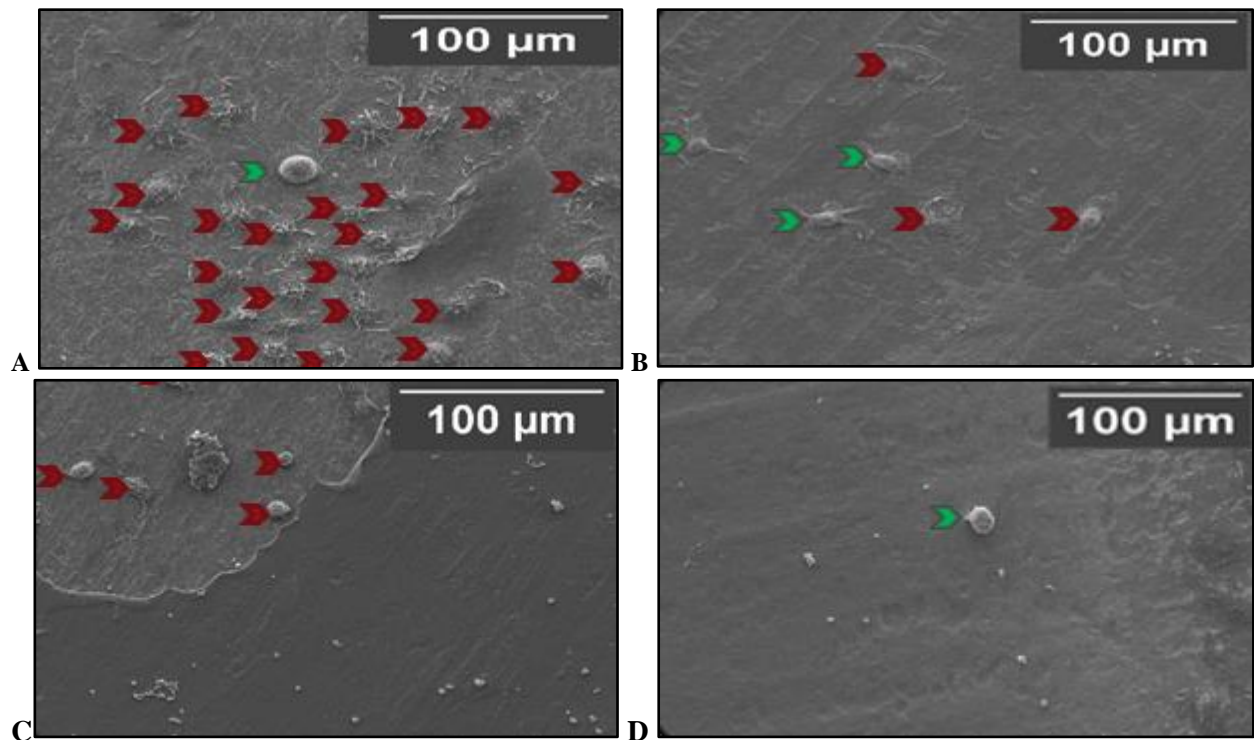
Figure 14: SEM images of (A) Ti foil, (B) TiO$_2$ nanotubes, (C) Chitosan-covered Ti foil, and (D) Chitosan-covered TiO$_2$ nanotubes 7 days after macrophage seeding. Green arrows indicate inactivated macrophages, red arrows indicated activated macrophages. Note the torn chitosan on (C), and the macrophage adherence and activation to the exposed Ti foil

This unexplained occurrence was observed only on Ti foil samples, with four of the imaged chitosan-coated Ti foil samples displaying torn chitosan in the center of the substrate. Additional depictions of these chitosan tears are shown in Fig. 15. TiO$_2$ samples only exhibited this disturbance on the corners where they had been handled by forceps prior to imaging.
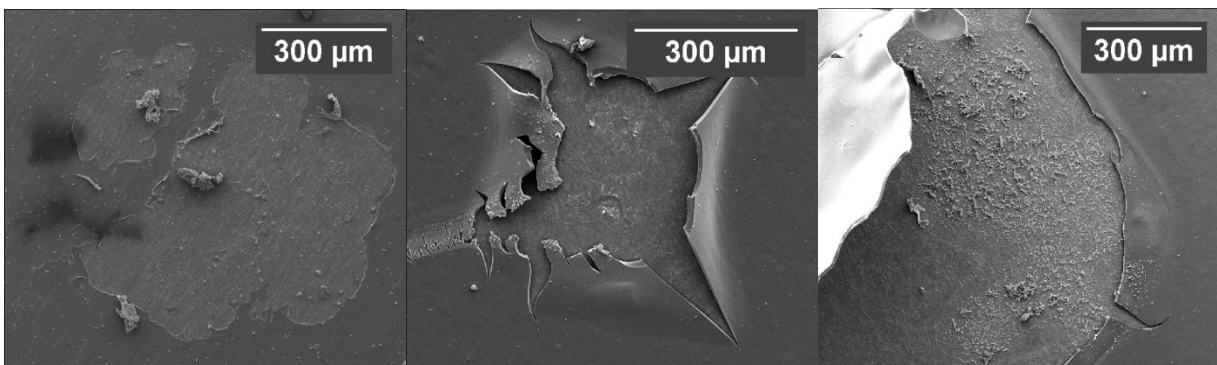
Figure 15: Examples of chitosan tears on chitosan-coated Ti foil samples

Further images in Fig. 16 show how the macrophages adhere to the TiO$_2$ nanotubes. These show the areas in which the filopodia actually adhered in the more activated macrophages. This also helps to show the state of the TiO$_2$ nanotubes after testing has been performed.
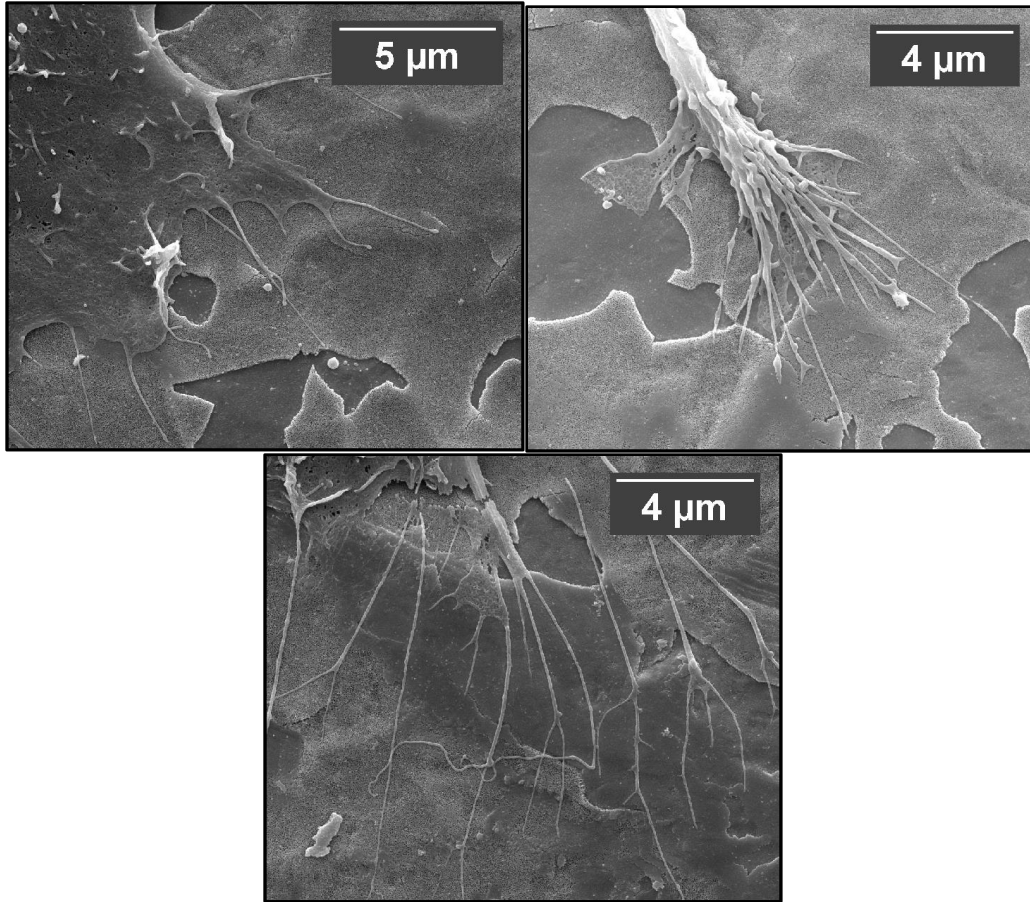
Figure 16: SEM images of macrophage adherence to TiO$_2$ nanotubes

In Fig. 16, there are also sections in which disturbances in the TiO$_2$ nanotubes are seen. This is further illustrated in Fig. 17, where the sectioning off and breaks in the TiO$_2$ nanotube shelves are clearly visible in contrast to the titanium beneath. These areas can be seen on most of the uncoated TiO$_2$ samples from both the Day 1 and Day 7 samples.
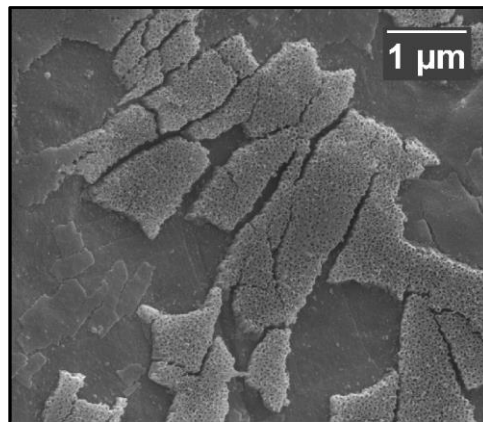
Figure 17: SEM image deterioration of TiO$_2$ nanotubes taken following testing

7.0 Analysis and Discussion

Through the results found in Chapter 6, an analysis was conducted to find patterns in observations and identify unexpected occurrences in the experimental testing. These observations have helped to form further hypotheses and decisions for continuations in testing, allowing for future recommendations to be formulated.

7.1 Analysis of Experimental Testing

Experimental testing allowed provided the data necessary for the design validation and the following analysis of these data expands upon the implications of these results. This is especially true for qualitative images taken using fluorescence imaging and SEM.

7.1.1 Titania Nanotubes

The TiO_2 nanotubes were a central part to the project and had some interesting results. The formulation of the nanotubes, though done properly, may not have been the correct diameter. This is due to the fact that the literature simply stated that the nanotubes should have a diameter of 70 nm in order to reduce macrophage activation. This is very general as the nanotubes have an inner and an outer diameter with varying shell thicknesses. The created nanotubes still did seem to reduce the macrophage adhesion and activation, as seen in Fig. 13 and Fig. 14, in comparison to the plain titanium foil. However, there were still instances of the macrophages activating on the TiO_2 nanotubes, as clearly seen in Fig. 16. This may have been in sections where the average diameter of the nanotubes was either significantly greater or less than the recommended 70 nm.

The sectioning off of the TiO_2 nanotubes seen in Fig. 17 was an unexpected observation on the uncoated samples. This may be linked to the handling of the samples during the fixation process. This was not seen in any of the chitosan-coated samples, though this is probably due to the lack of visibility through the hydrogel. The reason behind the nanotube failure should be further investigated, especially as the attachment of the chitosan hydrogel may be incredibly dependent upon it. Losing TiO_2 nanotubes also brings the problem of having loose particles in the body, which has the high potential for creating a further immune response. This can be extremely detrimental to the anti-inflammatory system and therefore must be avoided. It can be assumed that this would not be very great of a problem so long as the nanotubes are coated in a hydrogel which would effectively prevent the nanotubes from becoming loose within the body, however it would be best to conduct further testing first to ensure there is no way for this to happen. The final product also probably would not have this problem is it is unique to the foil being bent during testing, however the stresses placed upon the actual biosensor would have to be analyzed to make sure there is no similar occurrence.

7.1.2 FITC Release Study

The FITC release from the PLGA nanoparticles successfully demonstrated the ability for the nanoparticles to release a molecule of a molecular weight of 389.38 g/mol for a duration of two weeks. In the final design of the anti-inflammatory system, dexamethasone will be loaded into the nanoparticles in place of FITC. Dexamethasone will also need to be tested for release but expected results should be very similar as its molecular weight is 392.46 g/mol, almost identical to that of FITC. As the molecular weights are marginally different there slight modifications to the amount of dexamethasone loaded into the nanoparticles may have to be made. However, there is no reason to suspect that large alterations will

be necessary. There may also be some further discrepancies on the size of the nanoparticles as they alter batch to batch. Different sizes may be tested in future studies depending upon the abilities of future labs.

This release study will also need to be performed with 1% chitosan hydrogel instead of 2% agarose gel, in order to more properly quantify the release in future testing. Once these alterations have been tested, preliminary *in vivo* testing may be able to begin.

7.1. 3 Macrophage Adhesion and Activation

From the fluorescence and SEM imaging it was clearly demonstrated that the chitosan-covered TiO_2 nanotubes possessed the least amount of macrophage activation after both 24 hours and 7 days. These qualitative data are critical as they validate the design concept that the combination of TiO_2 nanotubes and 1% chitosan hydrogel would have an inhibitory effect on macrophage activity, and thus the subsequent recruitment of other cells to the biosensor and the eventual development of fibrotic scarring.

The effect of the chitosan hydrogel on macrophage behavior was also apparent, as all chitosan-covered samples demonstrated reduced macrophage adhesion and activation in comparison with their non-chitosan counterparts. The discrepancy between the two sample types, chitosan-covered and non-chitosan is most clearly evident in the day 7 samples in Fig. 14, evidencing the ability of chitosan to have an anti-inflammatory effect for the desired duration of time.

The critical difference in macrophage activity on chitosan-covered Ti foil and chitosan-covered TiO_2 nanotubes was the tearing of the hydrogel on the former. Multiple samples of chitosan-covered Ti foil possessed disturbances in the hydrogel layer, as depicted in Figs. 14 and 15. Macrophages gravitated towards the areas where these disturbances had occurred, adhered to and activation on the exposed foil. The reason for this discrepancy has not been determined, and suggestions for future analysis and testing are discussed in Section 7.2 below.

7.2 Future Recommendations

The anti-inflammatory system design of this project demonstrated potential for use in subcutaneous biosensor applications based upon its ability to reduce macrophage activity and maintain an extended release profile, but further work is needed to ensure its success. Initial considerations include alterations to the testing parameters. In terms of the nanoparticle release study, it is recommended that the test is performed with the hydrogel selected for the specific design, 1% chitosan, rather than 2% agarose. Prior to *in vivo* testing, dexamethasone must be loaded into the nanoparticles and a release study performed on them. A release study to failure should also be conducted to determine the full potential of the nanoparticles.

After the testing has moved *in vivo* to initial mouse testing, further areas for improvement can be suggested. The 1% chitosan hydrogel should be characterized, preferably utilizing an AFM, in order to determine the mechanical properties and adhesion of the chitosan when it has been dried on the TiO_2 nanotubes. In order to undergo insertion, the chitosan hydrogel will need to be analyzed for shear stress when attached to the TiO_2 nanotube-biosensor, and possibly modified to ensure that the hydrogel will stay intact. A more effective means of applying the chitosan in an even and fully-coating manner should be investigated.

Throughout the course of this study, additional questions were raised on the adherence of the chitosan hydrogel to the Ti Foil in comparison to its adherence to the TiO$_2$ nanotubes; however, due to time limitations it was not possible to investigate this issue further. For future studies, the tears in the chitosan hydrogel that appeared on the Ti foil should be further examined. It is hypothesized that the TiO$_2$ nanotubes help the chitosan to adhere more properly as the chitosan is able to slightly enter the tubes, thus providing better anchorage to the surface, however additional testing should be performed to prove or disprove this hypothesis. Other surface modifications to the Ti can also be investigated to see the different possibilities of chitosan adhesion. These additional surface modification considerations may be essential if future testing of a TiO$_2$ nanotube biosensor reveals weakened sensing capabilities.

Further items for investigation include the damage to the TiO$_2$ nanotubes observed in the Fig. 17. Even though this occurrence might only be found on the foil and will not be observed on the actual biosensor, it should still be tested to ensure that the hydrogel adheres properly and the nanotubes do not become loose within the body. Additional observations on the TiO$_2$ nanotubes were made during testing and could be investigated further; however, they are not discussed outside of Appendix H as they were not excessively pertinent to this project.

This possible occurrence of altered biosensor sensitivity should be investigated in addition to all of the aforementioned recommendations. It is recommended that the metabolic biosensor be made of titanium and then anodized as by the protocol in Appendix A to form TiO$_2$ nanotubes on the surface of the sensor. The sensor must then be tested, without any sort of coating, *in vitro* and *in vivo* to ensure functionality. After the sensor has been proven to work effectively and efficiently, further testing with hydrogel and drug-release systems can be performed to find the optimal coating layer so as to retain high performance abilities of the biosensor. When the system is fully completed and all components have been tested, more extensive *in vivo* studies can begin. During *in vivo* studies, the entire inflammatory system can then be analyzed as opposed to just the macrophages. It would be beneficial to then conduct macrophage activation testing using cytokine levels as opposed to the visual observations used in this project. It is the hope that after this testing has been done, this anti-inflammatory system may be able to be adopted into wide-spread use, thus completing the objectives.

8.0 Conclusion

To summarize, the first-generation MQP design of TiO$_2$ nanotubes, 1% chitosan hydrogel, and PLGA nanoparticles qualitatively demonstrated an ability to reduce macrophage adhesion, inhibit macrophage activation, and maintain a release profile of pharmaceutical compounds for two weeks. Although there are areas to be considered for additional testing, as discussed above in Section 7.2, the data presented above suggest that this anti-inflammatory design has a strong potential for use as a subcutaneous biosensor that generates a reduced inflammatory response and delays the development of fibrotic scarring by inhibiting macrophage activity, ultimately extending the functional lifetime of the device.

9.0 Acknowledgements

10.0 References

J Anderson, (2001). Biological responses to materials. *Annual Review of Materials Research*. vol. 31(1). pp. 81–110.

N Atta, A Galal, S. Ali, (2011). *Nanobiosensor for Health Care*.

K. Brammer et al, (2011) *Biomaterials Science and Engineering*. pp. 193-210.

T Butterfield, et al. (2006). The dual roles of neutrophils and macrophages in inflammation: A critical balance between tissue damage and repair. *Journal of Athletic Training*. vol. 41(4). pp. 457-465.

L Chamberlain, et al. (2011).Macrophage inflammatory response to TiO_2 nanotube surfaces. *Journal of Biomaterials and Nanobiotechnology*. vol. 2(3). pp. 293.

V Chenna, C Hu, D Pramanik, et al. (2011). A Polymeric Nanoparticle encapsulated Small-Molecule Inhibitor of Hedgehog Signaling (NanoHHI) Bypasses Secondary Mutational Resistance to Smoothened Antagonists. *Mol Cancer Ther,* vol. 11. pp. 165-173.

F Danhier, E Ansorena, JM Silva, R Coco, A Le Breton, V Preat, (2012). PLGA-based nanoparticles: An overview of biomedical applications. *Journal of Controlled Release.* vol. 161. pp. 505-522.

R Doong, H Shih, (2010). Array-based titanium dioxide biosensors for radiometric determination of glucose, glutamate, and urea. *Biosensors and Bioelectronics.* vol. 25(6). pp. 1439-1446.

M Hamidi, A Azadi, P Rafiei, (2008). Hydrogel nanoparticles in drug delivery. *Advanced Drug Delivery Reviews.* vol. 60(15). pp. 1638-1649.

D Higgins, et al. (2009). Localized immunosuppressive environment in the foreign body response to implanted biomaterials. *American Journal of Pathology*. vol. 175(1). pp. 161-170.

R Jayant, R Srivastava, (2007). Dexamethasone release from uniform sized nanoengineered alginate

      microspheres. *Journal of Biomedical Nanotechnology*.vol. 3, pp. 245-253.

S Leibovich, R Ross, (1975).The role of the macrophage in wound repair. A study with hydrocortisone

      and antimacrophage serum*. The American Journal of Pathology*. vol. 78(1). pp. 71-100.

R Muzzarelli, (2000) Chitin and Chitosan Hydrogels. *Handbook of Hydrocolloids.* pp. 849-888.

J Oliveira, I Leonor, R Reis,(2005). Preparation of Bioactive Coatings on the Surface of Bioinert

      Polymers through an Innovative Auto-catalytic Electroless Route. *Key Engineering Materials,* pp.

      284-286, 203-207.

 ProSono, (2006). Principles of the Inflammatory Response.

A Rajyalakshmi, B Ercan, K Balasubramanian, T Webster, (2011). Reduced adhesion of macrophages on

      anodized titanium with select nanotube surface features. *International Journal of Nanomedicine.*
      vol. 6. pp. 1765-1771.

C Sorg, (1991). Macrophages in acute and chronic inflammation. *Chest.* vol. 100(3). pp. 173-175.

S Vaddiraju, I Tomazos, D Burgess, F Jain, F Papadimitrakopoulos, (2010). Emerging synergy between
      nanotechnology and implantable biosensors: A review. *Biosensors and Bioelectronics,* vol.25
      (7). pp. 1553-1565.

J Wang, (2001). Glucose Biosensors: 40 years of Advances and Challenges. *Electroanalysis,* vol. 13(12).

      pp. 983-988.

X Wang, E Wenk, X Hu, G Castro, M Lorenz, X Wang, D Kaplan, (2007). Silk coatings on PLGA and

      alginate microspheres for protein delivery. *Biomaterials,* vol. 28. pp. 4141-4169.

N Wisniewski, M Reichert, (2000). Methods for reducing biosensor membrane biofouling. *Colloids and*
      Surfaces B: Biointerfaces. vol. 18(3). pp. 197-219.

E Yoo, S. Lee, (2010). Glucose biosensors: an overview of use in clinical practice. *Sensors*. vol. 10. pp.
      4558-4576.

Z Zanzan, et al. (2008). Direct electrochemistry and electrocatalysis of horseradish peroxidase
      Biosensors and Bioelectronics, vol. 23 (7).pp. 1032-1038

Appendices

Appendix A: Anodization of Titanium Foil

Adapted from: Eugen Panaitescu of the Northeastern University Department of Physics

Materials
- 0.127mm annealed 99% Ti foil
- DI
- Isopropanol
- 0.25M Hydrofluoric Acid

Procedure

Titanium Foil Preparation
1. Cut foil into 3x4 cm
   a. One 4x4 cm sample and two 3x4 cm samples
2. Press cut samples to flatten
   a. Using Carver Laboratory Press
   b. Only did one sample (left unwanted divots)
3. Ultrasonically clean in isopropanol for *15 mins*
4. Air dry with pressurized hose
5. Rinse with DI
6. Air dry with pressurized hose

Anodization
1. Anodize Ti sample for *45 mins* at 15 V
   a. In 0.25M HF
   b. Distance between cathode and anode was 5 cm
2. Rinse completed sample in DI
3. Rinse in isopropanol
4. Ultrasonically clean in isopropanol for *15 mins*

Notes:
- Have samples as flat as possible so distance between cathode and anode is equal
- Be consistent with distance between cathode and anode
- Do not have Ti foil sit in HF before voltage is applied
  - Oxidation will occur
- Sterilize samples before cell use

Appendix B: Image J Data

For both the inner and outer diameters, the average cross-section was taken. For each of the odd numbered diameters, the largest diameter was taken from an individual tube, with the even numbered diameters being the smallest diameter from the same tube. This allows for the average diameter of all the tubes to have been taken. This was necessary due to the differences in cross-sectional shape.

Inner Diameter	Length (nm)	Outer Diameter	Length (nm)
1	35.373	1	67.303
2	32.093	2	63.264
3	40.823	3	65.825
4	30.388	4	73.919
5	44.012	5	74.011
6	37.474	6	60.686
7	51.479	7	51.346
8	47.705	8	59.595
9	45.955	9	69.5
10	30.478	10	53.304
11	52.53	11	58.415
12	30.478	12	47.36
13	41.717	13	71.534
14	30.343	14	62.044
15	52.996	15	74.837
16	41.848	16	63.156
17	53.227	17	66.486
18	46.31	18	52.918
19	46.575	19	57.377
20	37.401	20	51.052
21	42.335	21	69.046
22	44.012	22	50.703
23	48.809	23	56.295
24	41.421	24	51.266
25	51.664	25	63.609
26	41.421	26	60.528
27	45.717	27	77.808
28	28.148	28	48.949
29	49.614	29	72.67
30	37.764	30	57.066
31	33.469	31	68.749
32	26.135	32	58.438
33	44.012	33	66.63
34	19.903	34	64.377

35	40.89	35	62.94
36	41.322	36	67.465
37	60.776	37	72.614
38	40.924	38	49.971
39	55.93	39	76.48
40	36.7	40	58.996
41	53.227	41	71.381
42	43.638	42	51.638
43	49.724	43	72.802
44	44.105	44	59.066
45	38.052	45	76.104
46	43.386	46	63.802
47	56.125	47	61.157
48	38.16	48	49.531
49	48.19	49	69.066
50	31.794	50	51.743
51	48.613	51	66.63
52	41.717	52	70.669
53	31.794	53	73.195
54	25.819	54	61.246
55	31.405	55	77.421
56	31.405	56	65.804
57	31.361	57	76.694
58	31.578	58	74.837
59	44.475	59	66.053
60	38.052	60	57.827
61	52.269	61	69.046
62	42.141	62	65.825
63	38.339	63	83.923
64	40.521	64	60.528
65	49.144	65	69.441
66	36.401	66	68.749
67	47.36	67	54.645
68	34.075	68	66.63
69	61.179	69	74.011
70	38.052	70	41.618
71	53.355	71	78.941
72	41.454	72	60.641
73	65.493	73	72.444
74	34.868	74	62.307
75	62.57	75	72.896

76	31.923	76	70.611
77	36.7	77	56.222
78	29.935	78	43.007
79	62.11	79	58.039
80	34.035	80	50.46
81	43.481	81	62.809
82	30.478	82	58.227
83	36.514	83	74.545
84	36.401	84	52.918
85	48.19	85	73.027
86	28.148	86	48.949
87	41.421	87	62.044
88	32.6	88	53.304
89	50.569	89	61.955
90	41.355	90	62.831
91	49.587	91	56.802
92	44.903	92	61.335
93	54.945	93	68.749
94	46.104	94	52.529
95	45.717	95	77.843
96	26.907	96	48.387
97	65.805	97	59.71
98	45.925	98	60.324
99	55.168	99	70.669
100	43.638	100	58.996
101	58.439	101	81.395
102	50.026	102	55.019
103	52.996	103	67.949
104	46.399	104	66.301
105	28.148	105	71.762
106	26.652	106	56.489
107	51.664	107	82.063
108	33.099	108	51.77
109	56.803	109	66.136
110	29.798	110	67.768
111	40.89	111	90.29
112	28.533	112	59.595
113	41.355	113	78.316
114	36.364	114	56.994
115	47.591	115	60.098
116	34.75	116	47.273

117	44.964	117	71.093
118	34.075	118	47.962
119	39.978	119	63.264
120	39.184	120	65.492
121	53.966	121	65.804
122	39.428	122	51.346
123	47.934	123	86.772
124	29.429	124	62.831
125	66.63	125	65.116
126	22.052	126	70.165
127	72.01	127	72.161
128	25.66	128	65.388
129	57.662	129	78.542
130	42.367	130	57.945
131	49.697	131	68.27
132	30.162	132	52.918
133	38.904	133	89.148
134	47.705	134	44.505
AVERAGE:	42.29765	135	66.301
		136	56.295
		137	50.703
		138	73.176
		AVERAGE:	63.80833

Appendix C: Fabrication of 1% Chitosan Gel

Adapted from: (Zanzan 2008)

Materials

- Chitosan powder (from shrimp shells, ≥75% deacetylated) from Sigma
- 2% Acetic Acid

Procedure

1. Dissolve chitosan in 2% acetic acid
2. Magnetic stir for 2 hrs at room temp (or until all powder has dissolved)
3. Store at room temperature

Appendix D: Nanoparticle Fabrication

Adapted from: (Chenna, 2011) performed by Dina Rassias:

Materials

- 5050 DLG mPEG 5000 (PLGA-PEG) (Evonik Corporation)
- Fluorescein 5(6)-isothiocyanate (FITC) ($\geq$ 90% HPLC from Sigma)
- Dichloromethane
- Acetone
- 4% polyvinyl alcohol
- DI water

Procedure

1. Dissolve 50mg of PLGA-PEG and 1mg of FITC in 400uL dichloromethane and 100uL acetone (8:2) in a round bottom flask
2. Add 2.5 mL of 4% polyvinyl alcohol to the resulting solution
3. Sonicate the solution for 3 mins at 20W , 4°C
4. Rotor-evaporate until complete evaporation of organic solvents.
5. Re-suspend in 3mL of ultrapure water.
6. Ultracentrifuge resulting suspension at 40,000 rpm for 45 mins
7. Wash the precipitated nanoparticle pellet 3X with ultrapure water
8. Re-suspend in ultrapure water (3ML), mild sonication
9. Centrifuge at 3000 rpm for 5 mins to remove any large aggregates
10. Flash freeze on dry ice and lyophilize
11. Re-suspend in ultrapure water with amount for desired concentration

Appendix E: FITC Release Study Protocol

Generated from: Suggestions by Prof. Jain of WPI

Materials
- Fluorescein 5(6)-isothiocyanate (FITC) (≥ 90% HPLC from Sigma)
- Dimethyl sulfoxide (DMSO) (for molecular biology ≥99.9% from Sigma)
- 10% PBS
- PLGA nanoparticles (Created by Dina Rassias)
- 2% agarose gel

Procedure

Standard Curve

Note: Keep FITC out of light as much as possible

1. Measure out 1μg of FITC with an equal amount of DMSO.
2. Dilute FITC solution with PBS to get a concentration of 10 μg/mL.
3. Dilute a portion of the 10 μg/mL with an equal amount of PBS to get a 5 μg/mL solution.
4. Repeat Step 3 to get 2.5 μg/mL, 1.25 μg/mL, 0.625 μg/mL, 0.3125 μg/mL, 0.15625 μg/mL, 0.078125 μg/mL, 0.039063 μg/mL, and 0.019531 μg/mL solutions.
5. To test the absorbance of the FITC, mix each sample by pitetting.
6. On the Nanodrop 2000 software, select BSA and Proteins, then AlexaFluor 488 for accurate readings.
7. Wash Nanodrop with PBS prior to testing and use PBS to calibrate the system.
8. Use Kim Wipe to remove PBS before adding 5 μL of lowest concentration, mixed FITC solution.
9. Run the sample, wipe off drop after test, and re-test the same concentration twice more, successfully testing the concentration in triplicate.
10. Wipe residual FITC drop from Nanodrop. Rinse with PBS, then re-zero with fresh PBS.
11. Repeat steps 7-9 for each concentration, making sure to mix each solution prior to each run.
12. Average the readings from Abs. 1 data for each concentration.
13. Plot average Absorbance readings versus the concentration and find the linear equation.

Release Study

1. Resuspend PLGA nanoparticles in PBS to create 25 mg/mL solution
2. Mix in a 1:1 ration with warm, liquid 2% agarose gel to create a 12.5 mg/mL nanoparticle solution (2% FITC concentration)
3. Fill glass vials #1, #2, #3 with 100 μL of agarose/nanoparticle solution, fill vials A, B, C with 150 μL of the solution. Cap and refrigerate vials at 4°C.
4. Leave in 4°C until solidified (~10 minutes)
5. Add 250 μL of 10% PBS to vials #1-3, add 300 μL in vials A-C.
6. Recap vials and place in 37°C for 24 hrs to simulate *in vivo* conditions.
7. Collect the PBS from each vial and place in separate, marked vials. Store in fridge at 4°C.
8. Replace the amount of PBS harvested from each vial with fresh PBS and place back in 37°C incubator.
9. Repeat steps 7-8 at time points 2, 3, 5, 7, 9, 11, and 13 days after initial PBS added to vials.

10. To test the absorbance of the FITC, mix each sample by pipetting.
11. On the Nanodrop 2000 software, select Proteins & Labels, then Alexa Fluor 488 for Dye 1 for accurate readings.
12. Wash Thermo Scientific Nanodrop 2000 Spectrophotometer with PBS prior to testing and use PBS to calibrate the system.
13. Use Kim Wipe to remove PBS before adding 5 μL of the Day 1, Vial 1, mixed FITC solution.
14. Run the sample, wipe off drop after test, and run Day 1, Vial 2.
15. Run the sample, wipe off drop after test, and run Day 1, Vial 3.
16. Wipe residual FITC drop from Nanodrop. Rinse with PBS, then re-zero with fresh PBS.
17. Repeat steps 7-9 for each day in vials 1-3, making sure to mix each solution prior to each run.
18. Repeat steps 14-19 with vials A-C.
19. Average the readings from Dye 1 Abs data for each day and each well volume (100 μL and 150 μL) and get the standard deviation.
20. Utilize the linear equation of the standard curve to get the concentrations of each day and each well volume, as well as the standard deviation.
21. Add concentrations to one another to get accumulation of the FITC over the days.
22. Plot the concentrations of each well type versus the day to get the cumulative release of the FITC from each of the well types, as well as the error bars in accordance to the standard deviations.

Appendix F: Hoechst and Phalloidin Staining

Adapted from: Yuan Yin and Professor Pins

Materials
- 10% PBS
- 2% formaldehyde
- 2% BSA
- Phalloidin
- PBS TWEEN
- Hoechst

Procedure
1. Aspirate media from wells, add in ~5 drops 10% PBS
2. Aspirate PBS after 5 minutes, add ~5 drops
3. Aspirate PBS after 5 minutes
4. Fix cells with ~7 drops of 2% formaldehyde, ensure they are covered
5. Leave for 60 minutes
6. Aspirate out the formaldehyde
7. Add ~5 drops PBS, leave for 5 min and aspirate
8. Repeat step 7 twice more
9. Add 200 μL of 2% BSA blocking agent to each sample (ensure it is covered)
10. Aspirate blocking agent after 5 minutes
11. Add freshly prepared Phalloidin stain (ensure sample is covered)
    a. Mix 5μL of stock Phalloidin stain with 200μL PBS TWEEN
12. Leave Phalloidin stain in wells for 15 min, then aspirate
13. Add freshly prepared Hoechst stain
    a. Mix 1μL of stock Hoechst stain with 1000μL PBS TWEEN
14. Leave Hoechst stain in wells for 5 min, then aspirate
15. Add normal PBS to each well (ensure sample is covered)
16. Cover well-plate with aluminum foil to block out light, store in 4°C fridge until imaging.
17. Image cells with a Leica Fluorescent Microscope system with image analysis software

Appendix G: Cell Fixation for SEM Imaging

Adapted from: Gregory Hendricks of UMASS Medical School

Materials
- 2.5% gluteraldehyde
- 10%, 30%, 50%, 70%, 85%, 95%, 100% ethanol
- Palladium/gold alloy

Procedure
1. For a 96 well plate, add 4 drops of 2.5% gluteraldehyde from a glass-pipette to each well to be fixed. Media should still be in the well.
2. Wait 10 minutes, then aspirate media/gluteraldehyde.
3. Add 5 drops gluteraldehyde to each well (ensure it covers the sample). Wait 15 minutes, then aspirate out.
4. Begin ethanol washes by adding ~5 drops of 10% ethanol to each well (ensure sample is covered).
5. After 10 minutes, aspirate and immediately add ~5 drops of 30% ethanol to each well separately (ensure the sample is never out of ethanol long enough to dry out.)
6. Repeat step 5 with a series of 50%, 70%, 85%, 95%, and 100% ethanol. (be especially careful when using ethanol above 70% as it dries very quickly)
7. Wash with 100% ethanol again and leave samples in 100% ethanol until point-drying.
8. Place each sample into a "marshmallow" or other penetrable basket designed for the point-drier. Make sure basket is marked and the bottom side of the sample has been scratched to indicate what side has macrophages. Make sure each basket remains submerged in 100% ethanol and the transfer of the sample from the well-plate to the baskets is quick.
9. Point-dry the samples in a AutoSamdri-815 critical point dryer.
10. After drying, mount samples on metal stubs to load into the SEM machine. Use carbon tape to attach them, ensure the scratched, bottom side of the sample is down. Make sure samples are noted to be able to tell the different sample types.
11. Load samples into a Cressington 208HR sputter coater.
12. Sputter samples with 4nm of palladium/gold alloy. Repeat two times to get a total thickness of 12nm of the alloy
13. Load the samples into an FEI Quanta 200 MKII FEG ESEM machine equipped with an Oxford-Link EDS system for imaging and analysis.
14. Image each sample.

Appendix H: Titania Nanotube Discoloration

In initial macrophage adhesion and activation studies, immortalized macrophages were seeded onto the four different sample types, including the TiO_2 nanotube samples. It was on these nanotube samples that there was a discrepancy with the macrophage adhesion. Fig. 18 below shows the pattern of macrophage adhesion to the lighter colored areas of the nanotubes sample.
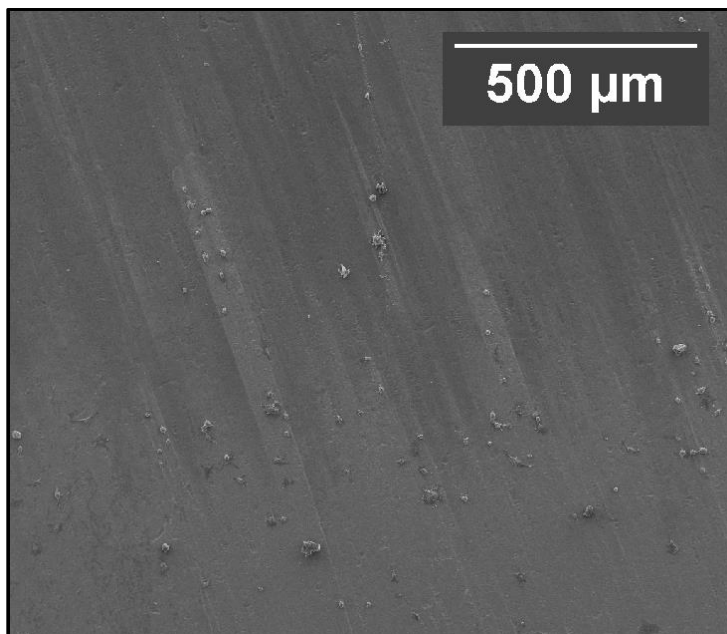

Figure 18: Immortalized macrophages adhered to the light areas of TiO_2 nanotubes on a Day 1 chitosan-coated TiO_2 nanotube sample.

In the image above there are obvious streaks of light and dark areas, with the macrophages only adhering to the lighter areas. When the physical sample was analyzed out of the SEM, it appeared that the different colorations corresponded to the color-changes of the titania. Due to the anodization process, the titania turned from gray to luminescent pink on some areas of the sample. When conferring with Northeastern University about this difference, they stated that the difference in color should not translate to a different color in the SEM, nor should it have different properties from the gray titania. This was not an isolated occurrence as it was observed on other samples. Fig. 19 demonstrates the findings of an uncoated, TiO_2 nanotube sample seeded with primary macrophages at Day 1, where this occurrence is also present. It is clearly visible that there are fewer macrophages adhered to the darker area, and all of which are in their spherical, inactivated state. This is different in comparison to the light areas, where there is much greater macrophage adhesion as well as activation.
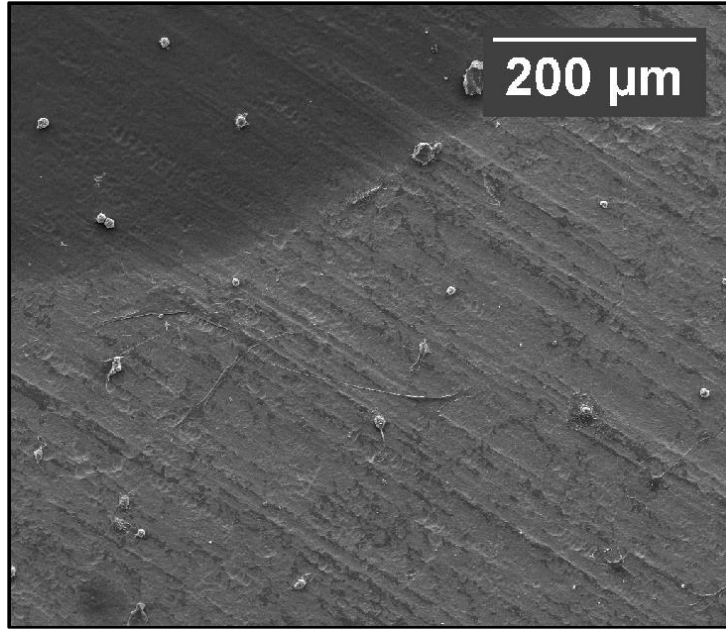
Figure 19: Light and dark areas of an uncoated TiO$_2$ nanotube sample seeded with primary macrophages on Day 1. Notice the inactivated macrophages on the dark areas and the activated ones on the light.

This continued on to Day 7 of the primary macrophage testing. Fig. 20 depicts macrophage avoidance of the darker area, and their activation solely in the lighter side of the partition.
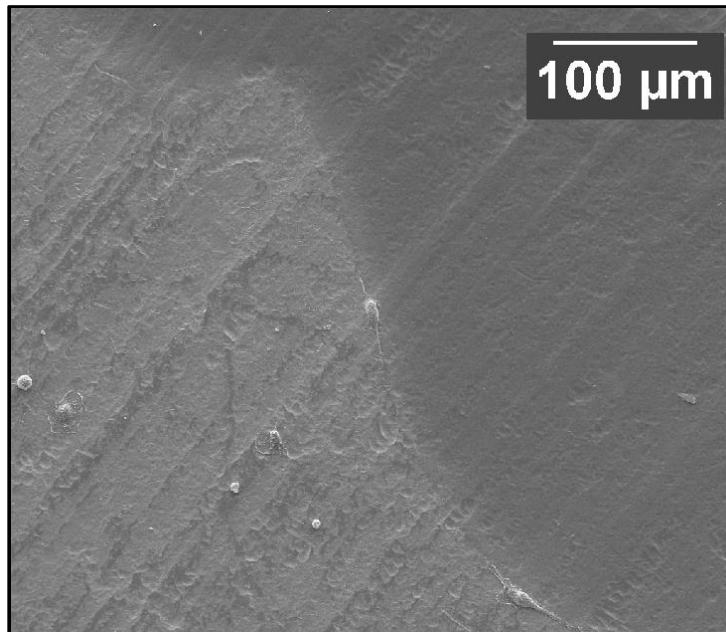

Figure 20: Day 7 primary macrophages on uncoated TiO$_2$ nanotubes.

This was an unexpected discovery, and one that was not explored further during the course of this project due to time constraints; future investigation into this subject is suggested. If the titanium can be anodized to have more of this darker area, inflammation may be further reduced as macrophage adhesion and activation is nearly eliminated.